

การใช้เก้าอี้แกว่งในเทอร์โมพลาสติกคอมพอสิต

นายวีระชัย เกียรติอุดมพันธ์

วิทยานิพนธ์นี้เป็นส่วนหนึ่งของการศึกษาตามหลักสูตรปริญญาวิศวกรรมศาสตรมหาบัณฑิต
สาขาวิชาวิศวกรรมเคมี ภาควิชาวิศวกรรมเคมี
คณะวิศวกรรมศาสตร์ จุฬาลงกรณ์มหาวิทยาลัย
ปีการศึกษา 2550
ลิขสิทธิ์ของจุฬาลงกรณ์มหาวิทยาลัย

USE OF RICE HUSK ASH IN THERMOPLASTIC COMPOSITES

Mr. Veerachai Kiet-udomphan

A Thesis Submitted in Partial Fulfillment of the Requirements
for the Degree of Master of Engineering Program in Chemical Engineering

Department of Chemical Engineering

Faculty of Engineering

Chulalongkorn University

Academic Year 2007

Copyright of Chulalongkorn University

Thesis Title USE OF RICE HUSK ASH IN THERMOPLASTIC
 COMPOSITES
By Mr. Veerachai Kiet-udomphan
Field of Study Chemical Engineering
Thesis Advisor Sirijutaratana Covavisaruch, Ph.D.

Accepted by the Faculty of Engineering, Chulalongkorn University in Partial
Fulfillment of the Requirements for the Master's Degree

..... Dean of the Faculty of Engineering
(Associate Professor Boonsom Lerthirunwong, Dr. Ing.)

THESIS COMMITTEE

..... Chairman
(Assistant Professor Vichitra Chongvisal, Ph.D.)

..... Thesis Advisor
(Sirijutaratana Covavisaruch, Ph.D.)

..... External Member
(Associate Professor Siriwan Srisorrachatr, Ph.D.)

..... External Member
(Ruengsak Thitiratsakul, Ph.D.)

4970582321: MAJOR CHEMICAL ENGINEERING

KEY WORDS: POLY(VINYL CHLORIDE) / RICE HUSK ASH / COMPOSITES /
MECHANICAL PROPERTY / THERMAL PROPERTY

VEERACHAI KIET-UDOMPHAN: USE OF RICE HUSK ASH IN
THERMOPLASTIC COMPOSITES. THESIS ADVISOR: SIRIJUTARATANA
COVAVISARUCH, Ph.D., 90 pp.

The purposes of this research are to develop the wood plastic composites (WPC) from poly(vinyl chloride) (PVC) and rice husk ash (RHA) as an alternative material substituting natural wood, and also to investigate the effects of particle sizes and the amount of RHA on the mechanical, thermal and physical properties of PVC/RHA composites. In this study, RHA was used as a filler. Rich in silica content, RHA was deemed an appropriate filler for WPC. RHA was grinded to particle sizes of 45, 75, 106, 180 and 250 μm and blended with PVC compound at 20, 40, 60 and 80 phr. Experimental results showed that the tensile, flexural and compressive modulus and compressive strength of the PVC/RHA composites increased with increasing in RHA contents. Both the tensile and the flexural strengths of the PVC/RHA composites tend to decrease with increasing RHA contents. This is due to the poor interfacial adhesion between the PVC and the RHA. With greater RHA contents, the impact energy decreased because the toughness of the PVC/RHA composites was decreased. For the thermal properties, the heat deflection temperature (HDT) and the glass transition temperature (T_g) of the PVC/RHA composites increased slightly with increasing RHA contents. This is because the RHA particles hindered the mobility of the PVC molecules. RHA had no significant effect on the decomposition temperature (T_d) of the PVC/RHA composites. Upon degradation, the residual solid weight of the PVC/RHA composites increased with greater RHA contents. The density and the rate of water absorption of the PVC/RHA composites also increased with higher RHA contents. With 20 phr, the PVC/RHA composites were dark grey in color. Further increase of the RHA content led to a change of color from dark grey to black. The particle sizes of the RHA had no significant effects on the modulus and strength under tensile, flexural and compressive stresses, the HDT, T_g , T_d , the density and the rate of water absorption while the impact energy increased with larger RHA particles. The small RHA particles yielded composites with a darker shade than those with larger RHA particles.

Department.....Chemical Engineering... Student's signature.....

Field of study....Chemical Engineering... Advisor's signature.....

Academic year2007.....

ACKNOWLEDGEMENTS

I would like to express my sincerest gratitude and deep appreciation to my advisor, Dr. Sirijutaratana Covavisaruch, for her kindness, invaluable supervision, invaluable guidance, advices, and encouragement throughout the course of this study and editing of this thesis.

I am very grateful to my committee members, who provided advices for the completion of this thesis. This includes, Asst. Prof. Dr. Vichitra Chongvisal, Chairman, from the Department of Chemical Engineering, Faculty of Engineering, Chulalongkorn University, Assoc. Prof Dr. Siriwan Srisorrachatr from Department of Chemical Engineering, Faculty of Engineering, Srinakharinwirot University and Dr. Ruengsak Thitiratsakul from the Petroleum Institute of Thailand (PTIT).

I am also grateful to Mr. Booranin Kamponpan from Nawaplastic Industries Company Limited for his consultation.

I am grateful for the partial research grant provided by the Asahi Glass Foundation, Japan. Nawaplastic Industries Company Limited, Thailand and Siam Power Supply Company Limited, Thailand are greatly appreciated for material support. Furthermore, thanks are extended to the Center of Excellence in Particle Technology and the Center of Excellence in Catalysis and Catalytic Reaction, Faculty of Engineering, Chulalongkorn University for facilitating the grinding and sieving equipment, and SDT analyzer respectively.

Additionally, I am grateful to everyone in the Polymer Engineering Laboratory, Chulalongkorn University, for their discussion and friendly encouragement. Moreover, I would like to thank everyone here. I feel so fortunate having a chance to learn here.

Finally, I would like to affectionately give all gratitude to the members of my family for their wholehearted understanding, encouragement, and patient support throughout my entire study.

CONTENTS

	PAGE
ABSTRACT (THAI)	iv
ABSTRACT (ENGLISH)	v
ACKNOWLEDGEMENTS	vi
CONTENTS	vii
LIST OF TABLES	xi
LIST OF FIGURES	xii
CHAPTER I INTRODUCTION	1
1.1 General Introduction	1
1.2 Objectives of the Research.....	3
1.3 Scopes of the Research	3
CHAPTER II THEORY	4
2.1 Composite Materials	4
2.1.1 Classification of Composite Materials.....	5
2.1.1.1 Particulate-Reinforced Composites	5
2.1.1.2 Fiber-Reinforced Composites	6
2.1.1.3 Laminar Composites	6
2.1.2 The Roles of Filler and Reinforcements	6
2.1.3 Properties of Filled and Reinforced Plastic	7
2.2 Theories of Adhesion.....	8
2.2.1 Interdiffusion.....	8
2.2.2 Electrostatic Attraction	8
2.2.3 Chemical Bonding	9
2.2.4 Mechanical Keying	9
2.3 Polymer Matrix	10
2.3.1 Poly(vinyl chloride), PVC	11
2.4 Rice Husk Ash (RHA)	13

	PAGE
2.5 Polymer Processing.....	14
2.5.1 Two-Roll Mill.....	14
2.5.2 Compression Molding.....	15
2.5.3 Extrusion.....	16
2.6 Polymer Characterizations.....	19
2.6.1 Mechanical Characterizations.....	19
2.6.1.1 Tensile Test.....	19
2.6.1.2 Flexural Test.....	20
2.6.1.3 Compressive Test.....	21
2.6.1.4 Impact Test.....	22
2.6.2 Thermal Characterizations.....	23
2.6.2.1 Heat Deflection Temperature (HDT).....	23
2.6.2.2 Dynamic Mechanical Analysis (DMA).....	24
2.6.2.3 Thermogravimetric Analysis (TGA).....	25
2.6.3 Morphology characterization.....	26
2.6.3.1 Scanning Electron Microscope (SEM).....	26
 CHAPTER III LITERATURE REVIEWS.....	 27
 CHAPTER IV EXPERIMENTS.....	 35
4.1 Materials.....	35
4.2 Experimental Procedure.....	36
4.2.1 Preparation of Rice Husk Ash (RHA).....	36
4.2.2 Processing of the PVC/RHA Composites.....	36
4.3 Testing and Characterizations.....	38
4.3.1 Mechanical Properties.....	38
4.3.1.1 Tensile Test.....	38
4.3.1.2 Flexural Test.....	39
4.3.1.3 Compressive Test.....	40
4.3.1.4 Notched Izod Impact Test.....	40

	PAGE
4.3.2 Thermal Properties.....	42
4.3.2.1 Heat Deflection Temperature (HDT).....	42
4.3.2.2 Dynamic Mechanical Properties.....	42
4.3.2.3 Thermogravimetric Analysis (TGA).....	43
4.3.3 Physical Characterizations.....	45
4.3.3.1 Density.....	45
4.3.3.2 Water Absorption.....	46
4.3.3.3 Outdoor Weathering Test.....	47
4.3.3.4 Microscopic Observation.....	47
CHAPTER V RESULTS AND DISCUSSION.....	49
5.1 Mechanical Properties of the PVC/RHA Composites.....	49
5.1.1 Tensile Properties.....	49
5.1.2 Flexural Properties.....	52
5.1.3 Compressive Properties.....	56
5.1.4 Impact Properties.....	58
5.2 Thermal Properties of the PVC/RHA Composites.....	61
5.2.1 Heat Deflection Temperature (HDT).....	61
5.2.2 Glass Transition Temperature (T_g).....	61
5.2.3 Thermogravimetric Analysis (TGA).....	63
5.3 Physical Properties of the PVC/RHA Composites.....	65
5.3.1 Density.....	65
5.3.2 Water Absorption.....	66
5.3.3 Outdoor Weathering Test.....	70
5.4 Morphological Characterizations of the PVC/RHA Composites.....	72
5.5 Cost Analysis of the PVC/RHA Composites.....	74
CHAPTER VI CONCLUSIONS AND RECOMMENDATIONS	
FOR FURTHER STUDIES.....	76
6.1 Conclusions.....	76
6.2 Recommendations for Future Study.....	77

	PAGE
REFERENCES	78
APPENDIX	84
Mechanical and Physical Characterizations.....	85
VITA	90

LIST OF TABLES

TABLE	PAGE
2.1 Properties of rigid PVC.....	12
2.2 Chemical constituents of rice husk ash.....	14
2.3 Thermal-transition temperatures of commercial polymers.....	24
5.1 Heat deflection temperature of the PVC/RHA composites	61
5.2 Glass transition temperature of the PVC/RHA composites.....	62
5.3 Cost analysis of the PVC/RHA composites.....	75

LIST OF FIGURES

FIGURE	PAGE
2.1 Continuous and discontinuous phase in a composite materials	4
2.2 Interfacial bonds formed	10
2.3 Two-roll mill	15
2.4 Compression molding	16
2.5 A simplified extruder diagram	17
2.6 Co-rotating twin screw extruder	18
2.7 Counter-rotating twin screw extruder	18
2.8 Stress-strain curve	20
2.9 Three-point bending test	21
2.10 Compressive test	22
2.11 Izod impact machine	23
2.12 Typical TGA thermogram	25
4.1 Raw materials	35
4.2 Grinding and sieving	36
4.3 Blending and processing	37
4.4 Tensile properties test	38
4.5 Flexural properties test	39
4.6 Compressive properties test	40
4.7 Notched Izod impact properties test	41
4.8 Heat deflection temperature test specimen	42
4.9 Dynamic mechanical analysis	43
4.10 Thermogravimetric analysis	44
4.11 Density measurement equipment	45
4.12 Water absorption test	46
4.13 Outdoor weathering test	47
4.14 Scanning electron microscope (SEM)	48
5.1 RHA contents on the tensile modulus of the PVC/RHA composites with various at 0 phr (●), 20 phr (■), 40 phr (◆), 60 phr (▲) and 80 phr (×) and different RHA particle sizes	51

FIGURE	PAGE
5.2 RHA contents on the tensile strength of the PVC/RHA composites with various at 0 phr (●), 20 phr (■), 40 phr (◆), 60 phr (▲) and 80 phr (×) and different RHA particle sizes.....	52
5.3 RHA contents on the flexural modulus of the PVC/RHA composites with various at 0 phr (●), 20 phr (■), 40 phr (◆), 60 phr (▲) and 80 phr (×) and different RHA particle sizes	54
5.4 RHA contents on the flexural strength of the PVC/RHA composites with various at 0 phr (●), 20 phr (■), 40 phr (◆), 60 phr (▲) and 80 phr (×) and different RHA particle sizes	55
5.5 The SEM micrographs of the PVC/RHA composites at (a) 20 phr 45 μm and (b) 60 phr 45 μm.....	56
5.6 RHA contents on the compressive modulus of the PVC/RHA composites with various at 0 phr (●), 20 phr (■), 40 phr (◆), 60 phr (▲) and 80 phr (×) and different RHA particle sizes	57
5.7 RHA contents on the compressive strength of the PVC/RHA composites with various at 0 phr (●), 20 phr (■), 40 phr (◆), 60 phr (▲) and 80 phr (×) and different RHA particle sizes	58
5.8 RHA contents on the notched Izod impact energy of the PVC/RHA composites with various at 0 phr (●), 20 phr (■), 40 phr (◆), 60 phr (▲) and 80 phr (×) and different RHA particle sizes	59
5.9 The SEM micrographs of the PVC/RHA composites at (a) 20 phr 45 μm and (b) 20 phr 180 μm.....	60
5.10 TGA thermograms of the PVC compound (●), RHA (+) and the PVC/RHA composites: 20 phr 45 μm (■), 20 phr 250 μm (□), 80 phr 45 μm (▲) and 80 phr 250 μm (△)	64
5.11 RHA contents on density of the PVC/RHA composites with various at 0 phr (●), 20 phr (■), 40 phr (◆), 60 phr (▲) and 80 phr (×) and different RHA particle sizes	66
5.12 Water absorption behavior of the PVC/RHA composites with particle size of 75 μm at 0 phr (●), 20 phr (■), 40 phr (◆), 60 phr (▲) and 80 phr (×).....	67

FIGURE	PAGE
5.13 Water absorption behavior of the PVC compound (●) and the PVC/RHA composites with RHA particle sizes of 45 μm (■), 75 μm (◆), 106 μm (▲), 180 μm (×) and 250 μm (+) at (a) 20 phr, (b) 40 phr, (c) 60 phr and (d) 80 phr.....	68
5.14 Water absorption of the PVC/RHA composites with various at 0 phr (●), 20 phr (■), 40 phr (◆), 60 phr (▲) and 80 phr (×) and different RHA particle sizes after immersion in water for 60 days	69
5.15 Porosity of the RHA particles	69
5.16 The appearance of the PVC/RHA composites before and after outdoor weathering test for 60 days	71
5.17 The SEM micrographs of the PVC/RHA composites at high magnification.....	73
5.18 The SEM micrographs of the PVC/RHA composites at low magnification.....	74

CHAPTER I

INTRODUCTION

1.1 General Introduction

Demand for wood increases with the growth of world population. Current statistics show the timber trade exceeds 1,687 million m³ in the world market [1]. Serious global concern is seen in the problem of nonrenewable logging of wood forests and the lack of replenishing forests. Hence, natural timber products are being partially substituted by new materials such as wood plastic composites (WPCs) to reduce the consumption of natural wood. The market demand for WPC in North America and Europe is increasing continuously. In 1995, the market demand in North America and Europe was about 50,000 tons per year. The market growth of WPC has averaged more than 25 percent since 1998. As compared with 700,000 tons per year in 2002, the predicted growth of WPC is 14 percent a year until 2010. From these statistics, the market growth of WPC has been the biggest building products in the section of plastic industry [2].

Typically, WPCs are produced by adding natural fiber as a filler in a polymer matrix such as polyethylene, polypropylene or poly(vinyl chloride) and then extruded or molded to the desired shape. During the process of WPC production, additives such as colorants, coupling agents, stabilizers, processing aids are added to improve the properties of the WPCs to the target areas of applications. WPCs have many advantages, they are splinter free and do not suffer insect damage. They resist weathering so they tend to have good dimensional stability and long life. Maintenance cost for WPCs is low. WPCs are made from environmental friendly materials which are also recyclable.

The growing concern for disposal of agricultural and industrial waste has prompted recent research endeavors to concentrate on converting these environmentally problematic wastes to useful industrial materials. In recent years, the development of WPCs using agricultural and industrial residues as reinforcing fillers has been gaining extensive attention. In Thailand, where rice is a major agricultural product for domestic consumption and also exporting, rice milling process generates large amount of by products such as rice husk and bran. The rice husk can be used as fuel for power generation in many small electricity generating plants. Rice husk ash (RHA) was obtained as waste created abundantly from these plants. There are two types of RHA namely, white rice husk ash (WRHA) and black rice husk ash (BRHA), they differ in inorganic impurities and residual carbon amounts, depending on the temperature at which the RHA was burnt. WRHA is obtained when RHA was burnt at a high temperature and excess oxygen. In contrast, BRHA is produced from burning RHA at low temperature. RHA is extremely low cost. Consisting predominantly of silica, it has a good potential to serve as a filler in thermoplastic composites.

Poly(vinyl chloride) (PVC) is a thermoplastic which softens, melts or flows when heated and hardens as it cools. So, it can be re-processed several times to form another product without destroying the original structure and properties. PVC is composed of large-sized molecules comprising of carbon (C), hydrogen (H) and chlorine (Cl) atoms. It is produced from natural products, which are 57 % by weight of common salt and 43 % by weight of petroleum or natural gas. In 1872, PVC was first made coincidentally during the laboratory experiments in Germany. After that, there were many laboratory-scale researches and tests of the product until 1930 when PVC was commercially developed in USA. It was produced as shock absorber seals and insulation, and then it was made avail to various applications. Rigid PVC was introduced in irrigation piping system during 1950, the PVC production and market then expanded rapidly [3]. At present, the total annual production of PVC worldwide is more than 30 million tons, and approximately more than 700,000 tons of PVC are produced annually in Thailand [4]. PVC possesses outstanding properties such as good strength, chemical stability, and stability at low temperatures, good weathering resistance, excellent electrical insulation and good surface properties. It is chemically inert and self extinguishing. PVC is very versatile. It can be used to produce plastic items ranging from soft to rigid products that are available at economic costs.

Examples of which include pipes, rainwater products with fittings, sheet, clear bottles, curtain rails, domestic window frames. The advantages of the use of RHA as the filler in PVC include reducing the WPC production cost, adding value to RHA and enhancing the utilization of agricultural waste in the plastic product industry.

The present study focused on the effects of RHA contents and its particle sizes on the mechanical, thermal and physical properties and the morphology of the PVC/RHA composites.

1.2 Objectives of the Research

This study is aimed to the followings:

- i) To develop thermoplastic wood plastic composites (WPCs) from PVC and rice husk ash (RHA).
- ii) To investigate the effects of RHA contents and its particle sizes on the mechanical, thermal and physical properties of the PVC/RHA composites.

1.3 Scopes of the Research

In this study, the composites were prepared from PVC using RHA as a filler. The particles of the RHA were sieved to sizes of 45, 75, 106, 180 and 250 μm . RHA of each size was dry blended with PVC compound at 20, 40, 60 and 80 phr, and then compression molded to prepare the PVC/RHA composite specimens. The effects of RHA contents and its particle sizes were investigated in terms of mechanical, thermal, and physical properties. The mechanical included tensile, flexural, compressive, and impact properties while the physical properties such as density, water absorption and weather resistant were performed. The thermal properties concentrated heat deflection temperature, glass transition temperature and decomposition temperature of the PVC/RHA composites. Microscopic observation of the PVC/RHA composites was carried out by using a scanning electron microscope (SEM).

CHAPTER II

THEORY

2.1 Composite Materials

Composite materials are materials which made up from two or more components and consist of two or more phases (heterogeneous) on a macroscopic scale. The main phase, known as matrix, is usually a continuous and often uniform phase. The matrix generally performs the function of a binder to transfer stress to the reinforcement and ensure their cooperative interaction. The other phase, generally acts as reinforcement, is a discontinuous phase surrounded by the matrix. The constituents can be organic, inorganic or metallic in various forms such as particles, platelets and rod as shown in Figure 2.1.

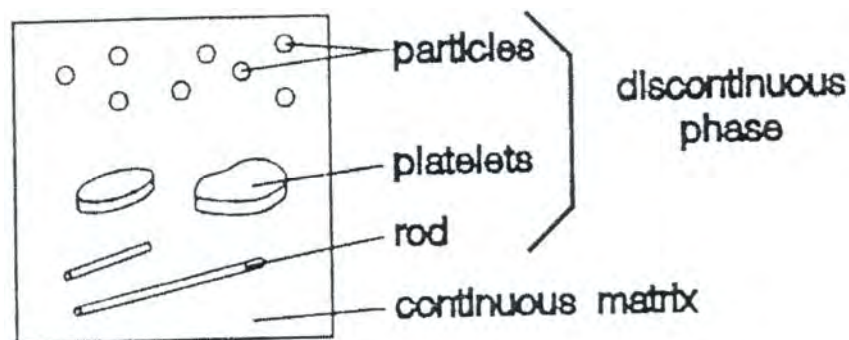


Figure 2.1 Continuous and discontinuous phase in a composite materials [5].

Polymeric composites comprise at least one type of polymer and other materials, such as organic or inorganic additives having certain geometries such as fibers, flakes, spheres, and particulates. Except, polymer blends are usually not classified as composites since the structural unit is formed at a microscopic level rather than a macroscopic one [5]. The additives may be continuous, e.g. long fiber or

ribbon; these are embedded in the polymer in regular geometric arrangement that extend throughout the dimensions of the product [6].

Many commercial polymer materials are composites. There are many reasons for using composite materials rather than the simple homogeneous polymers. Some of these reasons are:

- i) Increased stiffness, strength, and dimensional stability
- ii) Increased heat deflection (or distortion) temperature
- iii) Increased toughness or impact strength
- iv) Increased mechanical damping
- v) Reduced permeability to gases and liquids
- vi) Modified electrical properties
- vii) Reduced cost.

The properties of composite materials are ascertained by the properties of the components, by the shape of the filler phase, by the morphology of the system, and by the nature of the interface between the phases. Thus a great variety of properties can be obtained with composites just by alteration of one of these items. An important property of the interface that can greatly affect mechanical behavior is the strength of the adhesive bond between the phases [7-8].

2.1.1 Classification of Composite Materials

Composite materials can be divided into three general classes according to reinforcement forms [7-8].

2.1.1.1 Particulate-Reinforced Composites

Particulate-reinforced composites consist of particles dispersed in a matrix. They are considered to be particles if all of their dimensions are roughly equal. Particulates can be any shapes, configurations or sizes. They may be powder, beads, rods, crystalline or amorphous. Particles may be metallic, ceramic, manmade, or natural materials. Concrete and wood particleboards are two familiar examples of particulate composites.

Generally, particles in polymer usually extend rather than reinforce the polymer. These are usually referred to as filled systems. Because filler particles are included for the aim of cost reduction rather than reinforcement, these composites are not generally considered to be particulate composites. Nonetheless, in some cases the filler will also reinforce the matrix material.

2.1.1.2 Fiber-Reinforced Composites

Fiber-reinforced composites are composed of reinforced fibers in a matrix. They contain reinforcements having lengths greater than their cross-sectional dimensions. They can be further divided into those containing discontinuous and continuous fibers. In discontinuous fibers case, the bond between the fibers and the matrix is broken at the fiber's ends, so the fibre carry less stress than at its middle part while in continuous fibers case, the fibre can carry stresses along its length.

2.1.1.3 Laminar Composites

Laminar composites consist of layers with different anisotropic orientations or of a matrix reinforced with a dispersed phase in form of sheets. When a fiber reinforced composite consists of several layers with different fiber orientations, it is called multilayer composite. Laminar composites provide increased mechanical strength in two directions and only in one direction, perpendicular to the preferred orientations of the fibers or sheets, the mechanical properties of the material are low.

2.1.2 The Roles of Filler and Reinforcements

The function of active filler can be attributed to several mechanisms. Some fillers form chemical bond with the material to be reinforced, such as carbon black produces crosslink in elastomers by means of radical reaction. Other fillers act mainly through the volume they take up. The chain molecules of the polymer to be reinforced cannot assume all the conformational positions that are basically possible. Moreover, it can be assumed that in certain zones around the filler particles the polymeric phase differs in structure and properties from the polymer matrix. The polymer segments attached to filler surfaces by primary or secondary valence bonds

in turn caused a certain immobilization of adjacent segment and circumstances permitting an orientation of the polymer matrix. The increase in glass transition temperatures observed in filled polymers, resulting from the limitations of mobility in the filler and polymer boundary zone, can be regarded as confirmation of this theoretical concept [9].

The zone direct to filler surface, whose structure would appear to be ordered, causes a stiffening of the material as a whole. Lower deformability and higher strength are also due to this composite nature. Uniform distribution of fillers is especially important, so that as many polymer chains as possible can be bound to the free filler surface. The free surface energy and the polarity of the bond between the filler and the matrix are important factors in this regard. Another mode of action of active fillers is from the fact that when the polymer molecules are subjected to mechanical stress, they can slide off the filler surface.

2.1.3 Properties of Filled and Reinforced Plastic

The main objectives in use of fillers are to lower cost of molding compounds and to select modification of the properties of a plastic. These can divide the fillers into two categories, inert or extender fillers and active or reinforcing fillers [10-11].

i) Extender Fillers: The use of extender fillers can result in the following changes in the properties of thermoplastics:

- Increase in density
- Increase in modulus of elasticity
- Increase in compressive and flexural strength (stiffening)
- Lower shrinkage
- Increase in hardness and improvement in surface quality
- Increase in heat deflection temperature
- Cost reduction.

ii) Reinforcing Fillers: The reinforcing fillers produce the following improvement in thermoplastics:

- Increase in tensile strength and tensile stress at break
- Increase in compressive and shear strengths
- Increase in modulus of elasticity and stiffness
- Increase in heat deflection temperature
- Lower shrinkage
- Improvement in creep behavior and bend-creep modulus
- Reduction in the viscoelastic yield under load
- Partial improvement in impact strength.

2.2 Theories of Adhesion

Adhesion can be attributed to four main mechanisms, which can occur at the interface either in isolation or in combination to produce the bond [12].

2.2.1 Interdiffusion

It is possible to form a bond between two polymer surfaces by the diffusion of polymer molecules on one surface into the molecular network of the other surface, as shown in Figure 2.2(a). The bond strength will depend on the amount of molecular entanglement and the number of molecules involved.

2.2.2 Electrostatic Attraction

Forces of attraction occur between two surfaces when one surface carries a net positive charge and the other surface a net negative charge as in the case of acid-base interactions and ionic bonding and coupling agents laid down on the surface of the fillers, as shown in Figure 2.2(b).

2.2.3 Chemical Bonding

A chemical bond is formed between a chemical grouping on the filler surfaces and a compatible chemical group in the matrix as seen in Figure 2.2(c). The strength of the bond depends on the number and type of bonds and interface failure must involve bond breakage. The chemical bonds may be covalent, metallic, ionic, etc., and in many cases are very strong. There are many examples of the interfacial bond strength being raised by localized chemical reactions, but it is often observed that a progressive reaction occurs which results in the formation of a brittle product.

2.2.4 Mechanical Keying

Some bonding may occur purely by the mechanical interlocking of two surfaces as illustrated in Figure 2.2(d). There may be contribution to the strength at the interfaces from the surface roughness of the fillers is possible if good wetting has occurred. The effects are much more significant under shear loading than for decohesion as a result of tensile stresses. Improved resistance to tensile failure may be achieved if re-entrant angles are present. Strength under all types of loading can be increased as a consequence of the increased area of contact.

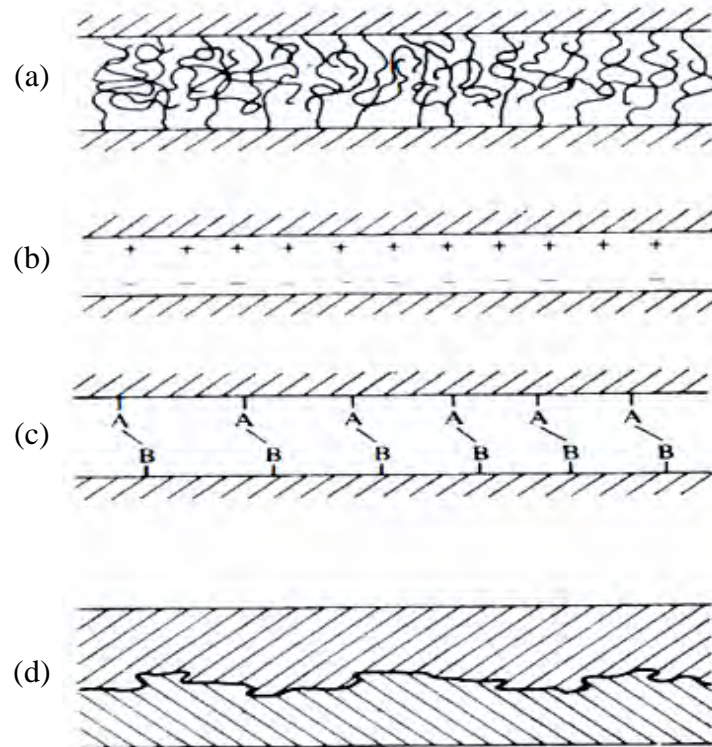


Figure 2.2 Interfacial bonds formed by Molecular entanglement following:

(a) Interdiffusion, (b) Electrostatic Attraction, (c) Chemical Bonding, and (d) Mechanical Keying [13].

2.3 Polymer Matrix

Various kinds of thermoplastic polymers are reinforced with reinforcements. Thermoplastic polymers are commercially divided into two classes, commodity thermoplastic and engineering thermoplastic.

i) Commodity plastics: In general, properties of the plastic are intermediate and the product has many applications. For example, polyethylene, polypropylene, polystyrene, poly(vinyl chloride), poly(ethylene terephthalate), etc.

ii) Engineering plastics: The engineering plastics are plastics applied to use for particular application. They have higher price than commodity plastics. Their outstanding properties allow them to compete successfully with other material such as

metals, ceramics, etc., for engineering application. They are strong, stiff, tough, abrasion-resistance, capable of withstanding wide ranges of temperatures, resistance to weather, chemicals, and other hostile condition. The engineering plastics include acrylonitrile-butadiene-styrene copolymer, polycarbonate, nylon, polyacetal, ultra high-molecular weight polyethylene, etc.

Because the commodity plastics such as poly(vinyl chloride) (PVC) have many advantages such as recyclability, cheap, etc., so PVC is used as the polymer matrix in this study.

2.3.1 Poly(vinyl chloride), PVC

PVC is a commodity thermoplastic. It is available in two general grades, rigid or unplasticized, and flexible or plasticized. Rigid-grade PVC is used as sheet, pipe, and window profiles, and for other molded parts. Flexible-grade PVC is obtained by blending PVC with low glass transition temperature (T_g) plasticizers. Application of plasticized PVC includes wire coating, upholstery, floor covering, film, and tubing. PVC decomposes at about 100 °C, which is far below its melting point of 150-200 °C. PVC degrades in the presence of light and UV. It has poor mechanical properties and a relatively low softening point, between 70 and 80 °C [14]. Properties of rigid PVC are shown in Table 2.1.

PVC resins can be produced by the free radical polymerization of vinyl chloride, $\text{CH}_2=\text{CHCl}$. The repeat unit of PVC polymer chain is $[-\text{CH}_2-\text{CHCl}-]$. The polymerization techniques which are used to produce PVC polymer, have three major methods namely, suspension polymerization (about 80% of total commercial PVC production), emulsion polymerization (about 10- 15%), bulk or mass and solution polymerization (about 10%) [14]. For suspension polymerization, vinyl chlorides are polymerized in an aqueous batch suspension. The benefit of this method is easier to control particle size and shape. Emulsion PVC resins are polymerized in the presence of water-soluble, free radical initiator and characterized by high polymerization rates leading to high molecular weight resins. This type of PVC is normally less expensive than other forms of PVC, but requires higher amount of lubricants. Bulk polymerized PVC resins are particles having very porous structure with a large surface. PVC resin

has poor mechanical properties and is low thermal stability. These disadvantages can be improved by incorporating additives that lead to various better properties of the PVC compound [15].

Table 2.1 Properties of rigid PVC [16].

Property	Rigid PVC
Specific gravity	1.32-1.44
Tensile strength (MPa)	37.92-55.16
Tensile modulus (GPa)	2.83
Flexural strength (MPa)	41.37-110.32
Flexural modulus (GPa)	2.41-4.14
Compressive strength (MPa)	68.95-75.84
Water absorption after 24 h (%)	0.1
Weather stability	Good for light colors

Various types of additives used in general for PVC products manufacturing can be summarized as follows [14,17]:

i) Plasticizers: To enhance the melt behavior of PVC resins and consequently improves the processability of PVC compounds. In addition, they help to convert hard, inherently brittle PVC resins into the compositions with varying degrees of softness and flexibility.

ii) Heat stabilizers and UV stabilizers: To increase properties of its tolerance to heat, sunlight and UV radiation to enhance the durability of the product, stability of shade of color and longer life of use.

iii) Lubricants: To prevent distortion of PVC shape in the process of molding mechanical form for various products. The lubricant enhances the flux of material and reduces surface friction between material and matrices or equipment in the process of shaping mechanical form.

iv) Impact Modifiers: To strengthen and enhance its tolerance to impact by modifying its properties to transfer the force of the material fabric.

v) Fillers: To reduce material cost and enhance certain properties, particularly the stiffness. Moreover, the fillers increase the amount of the texture of the substance and gross weight of the materials. However, the addition of fillers may have effect on reducing the tensile strength, elongation at break, impact strength, and on increasing the hardness and density of the material.

PVC plastics exhibit good mechanical toughness, resistance to weathering, and electrical insulating properties. Although they have a high-melt viscosity and require heat stabilizers, they are fairly easily processed by extrusion, calendaring, milling, or injection-molding techniques. PVC materials have excellent resistance to inorganic acids, alkalis, water, and very good resistance to oxygen and ozone degradation, and an important attribute of PVC is its low flammability. This also is a consequence of its high chlorine content [18-19].

2.4 Rice Husk Ash (RHA)

The burning of rice husk in air always leads to yield two types of ash, black rice husk ash (BRHA) and white rice husk ash (WRHA), which varies from gray to black depending on inorganic impurities and unburned carbon amounts [20-21]. BRHA which is created from burning of rice husk at low temperature is high amount of carbon, about 5-30 %. WRHA is produced from burning at higher 600 °C temperature, and excess air. The chemical compositions of RHA are shown in Table 2.2. RHA is an excellent insulator, having low thermal conductivity, high melting point, low bulk density and high porosity [22].

Table 2.2 Chemical constituents of rice husk ash [23].

Compositions	Quantity (% by weight)
SiO ₂	86.9 – 97.3
K ₂ O	0.58 – 2.5
Na ₂ O	0.0 – 1.75
CaO	0.2 – 1.5
MgO	0.12 – 0.96
Fe ₂ O ₃	0.0 – 0.54
P ₂ O ₅	0.2 – 2.85
SO ₃	0.10 – 1.13
Cl ₂	0.0 – 0.42

2.5 Polymer Processing

The manufacture of thermoplastic composites is often a two-step process, compounding and forming [24]. The fillers and additives are mixed with the molten polymer and then formed into a product by using many techniques such as compression molding, extrusion, etc.

2.5.1 Two-Roll Mill

Before a polymer can be used to make product, it is usually necessary to mix it with ingredients, which serve a variety purpose. The simplest and basic machine for intensive mixing is a two roll mill as shown in Figure 2.3. The two roll mill is comprised of a pair of rollers with axes horizontally disposed to each other, giving a vertical nip between them. The polymer matrix and additives are subject to high shear in the nip as the rolls rotate in opposite directions.

The technique of this machine is to pass the appropriate loading of matrix material, usually raw polymer, through the nip a few until it warms up, softens, and forms smooth band around one of the rolls. This process is assisted manually by

cutting the band with a knife from one edge to two-third to three-quarters of its width, so that a flap of it is formed can be folded to the side. By cutting and folding many times from both sides, good distribution and dispersion are achieved [25].



Figure 2.3 Two-roll mill [26].

2.5.2 Compression Molding

Molding processes are those in which a finely divided plastic is forced by the application of heat and pressure to flow into, fill and conform to the shape of a cavity (mold). One of the oldest methods of polymer processing is compression molding as shown in Figure 2.4. Here the polymer is put between stationary and movable members of a mold. The mold is closed and heat and pressure are applied so that the material becomes plastic, flows to fill the mold, and becomes a homogeneous mass. The necessary pressure and temperature vary considerably depending upon the thermal and rheological properties of the polymer. For a typical compression-molding material they may be near 150 °C and 1000-3000 psi [27]. A slight excess of material is usually placed in the mold to insure its being completely filled. The rest of the polymer is squeezed out between the mating surfaces of the mold in a thin, an easily removed film known as flash.

If a thermoplastic material is being molded, the mold is cooled, the pressure released, and the molded article removed. If a thermosetting material is used, the mold need not be cooled at the end of the molding operation or cycle, as the polymer will have set up and can no longer flow or distort.

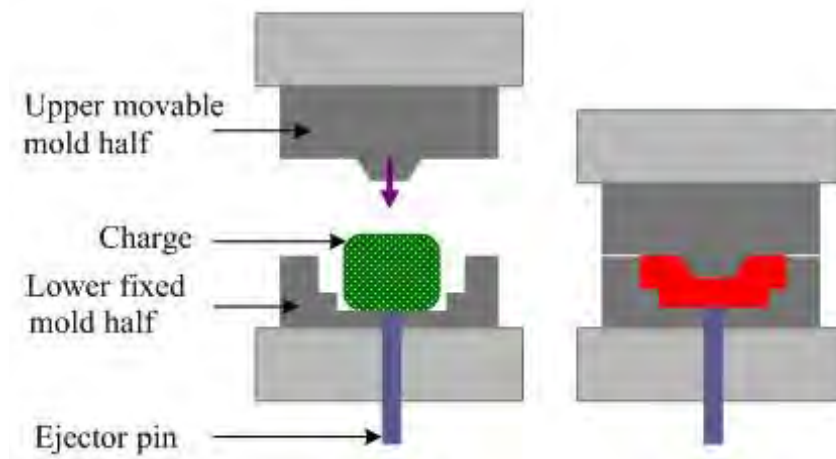


Figure 2.4 Compression molding [28].

2.5.3 Extrusion

Extrusion is one of the most common processes in polymer industry for mixing, compounding or reacting polymeric material. It has been classified into two types depending on the number of screw in extruder, single screw extruder and twin screw extruder. A simplified extruder diagram is shown in Figure 2.5. The screw is generally divided into three sections namely the solids conveying section, the compression or melting section, and the metering or pumping section. The most widely used type is the single screw extruder. Twin screw extruder is also used when superior mixing or conveying is important [25,29].

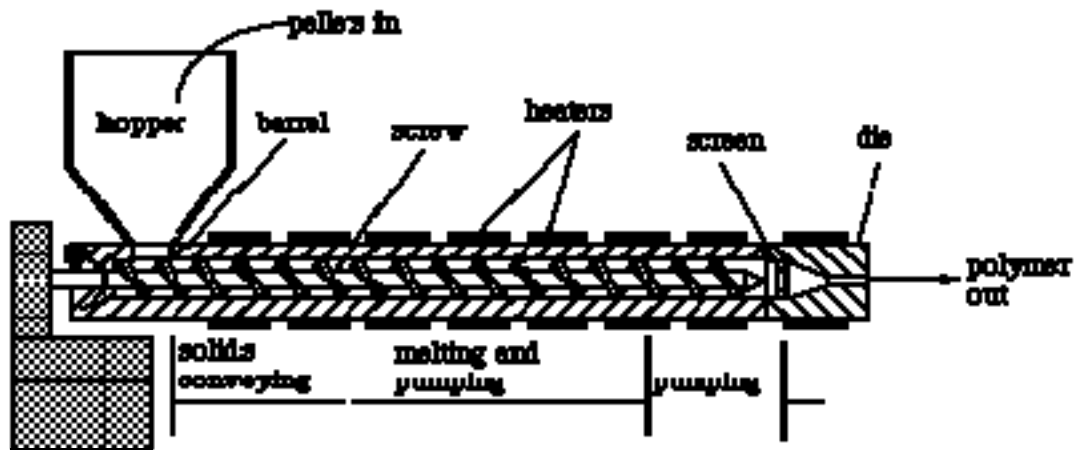


Figure 2.5 A simplified extruder diagram [29].

Twin screw extruder is divided into co-rotating and counter rotating types. As the names indicate, the difference is in whether the two screws rotate in the same or in opposite direction, i.e. both clockwise or counterclockwise, or one in each sense. Twin screw extruder acts as positive displacement pumps with little dependence on friction, and this is the main reason for their choice for heat sensitive materials such as PVC [25].

i) Co-Rotating Twin Screw Extruder: The co-rotating twin screw extruder transfers the melt from the screw channel of one screw to the other screw. The conveying mechanism, drag force is comparable to that found in the single screw extruder. By being transferred from one screw channel to another, the melt does follow a longer path and is subjected to higher shear. The co-rotating twin screw extruder finds application primarily in compounding. Figure 2.6 presents the co-rotating twin screw extruder.

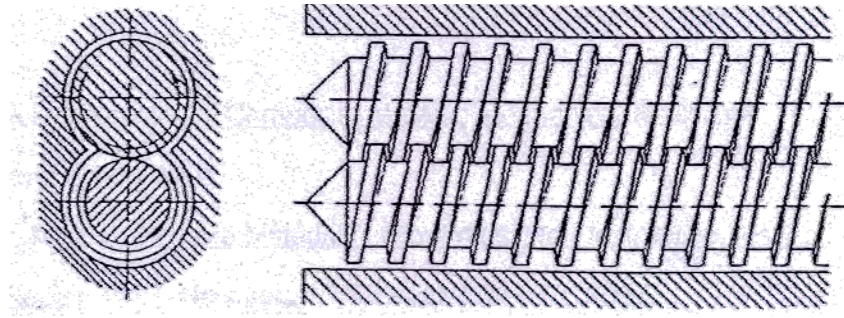


Figure 2.6 Co-rotating twin screw extruder [25].

ii) Counter-Rotating Twin Screw Extruder: Each screw segment forms a close chamber that conveys the melt material from the hopper to the end of the screw without any change with neighboring chambers. Drag forces are not needed for this conveying, with the result that little dispersion induced heating occurs. Heating occurs largely via the heater bands on the barrel, which can be controlled and permit gentle heating of sensitive materials. While this conveying and melting mechanism assures well controlled, gentle handling of the material, the melt is usually inhomogeneous and insufficiently plasticated so that the use of mixing elements is also recommended here. Figure 2.7 shows the counter-rotating twin screw extruder.

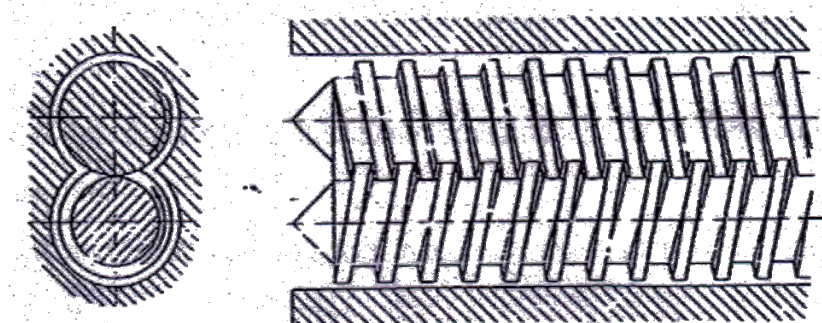


Figure 2.7 Counter-rotating twin screw extruder [25].

2.6 Polymer Characterizations

2.6.1 Mechanical Characterizations

2.6.1.1 Tensile Test

The tensile test is probably the most fundamental type of the mechanical test. The material will react to forces being applied in tension. As the material is being pulled, its strength along with how much it will elongate. When the material is pulled until breaks, complete tensile profile will be obtained as shown in Figure 2.8. A curve will result showing how it reacted to the forces being applied. In the initial portion of the tensile test, the relationship between the applied load and the elongation the specimen exhibits is linear. In this linear region, the line obeys the relationship defined as Hooke's Law where the ratio of stress to strain is a constant as shown in Equation (2.1).

$$E = \frac{\sigma}{\varepsilon} \quad (2.1)$$

where E = modulus of elasticity or Young's modulus
 σ = stress
 ε = strain

The modulus of elasticity is a measure of the stiffness of the material. If a specimen is loaded within this linear region, the material will return to its exact same condition if the load is removed. At the point that the curve is no longer linear and deviates from the straight-line relationship, Hooke's Law no longer applies and some permanent deformation occurs in the specimen. This point is called the elastic limit or proportional limit. From this point on in the tensile test, the material reacts plastically to any further increase in load or stress. It will not return to its original, unstressed condition if the load were removed.

The ultimate tensile strength (UTS) is the maximum load the specimen sustains during the test. The UTS may or may not equate to the strength at

break. This all depends on what type of material you are testing such as brittle, ductile, or a substance that even exhibits both properties [30].

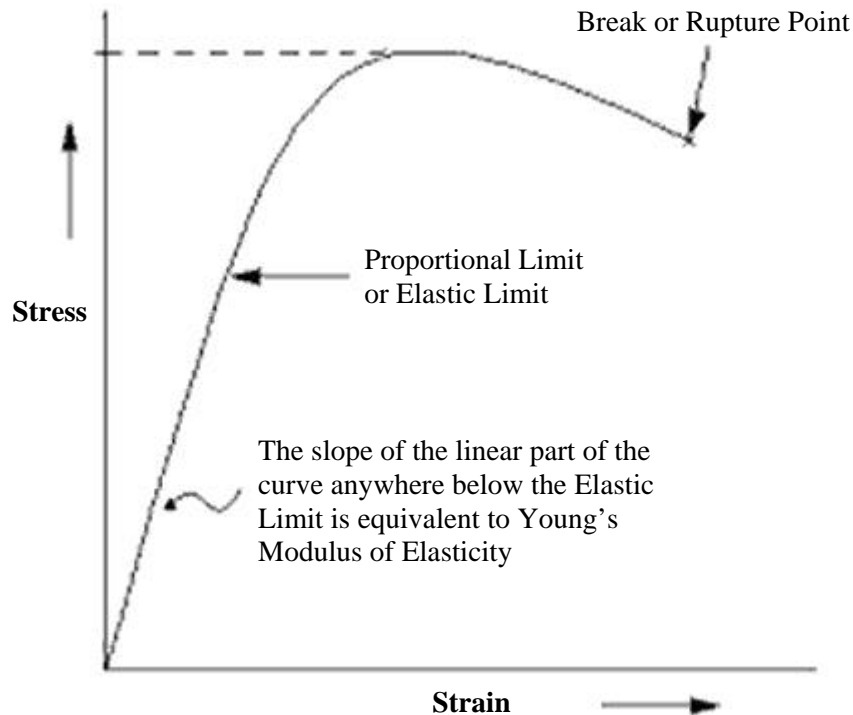


Figure 2.8 Stress-strain curve [30].

2.6.1.2 Flexural Test

The flexural test measures behavior of the materials subjected to simple beam loading. It is also called a transverse beam test with some materials. Maximum stress and maximum strain are calculated for increments of load. Results are plotted in a stress-strain diagram. Flexural strength is defined as the maximum stress in the outermost fiber. This is calculated at the surface of the specimen on the convex or tension side. Flexural modulus is calculated from the slope of the stress versus deflection curve. If the curve has no linear region, a secant line is fitted to the curve to determine slope. The flexural test produces tensile stress in the convex side of the specimen and compression stress in the concave side. This creates an area of shear stress along the midline. To ensure the primary failure comes from tensile or compression stress the shear stress must be minimized. This is done by controlling the

span to depth ratio, the length of the outer span divided by the height (depth) of the specimen. For most materials $S/d=16$ is acceptable. Some materials require $S/d=32$ to 64 to keep the shear stress low enough. Flexure testing is often done on relatively flexible materials such as polymers, wood and composites. There are two test types; 3-point bending and 4-point bending. In a 3-point test the area of uniform stress is quite small and concentrated under the center loading point. In a 4-point test, the area of uniform stress exists between the inner span loading points (typically half the outer span length) [31-32]. Figure 2.9 demonstrates the three-point bending test.

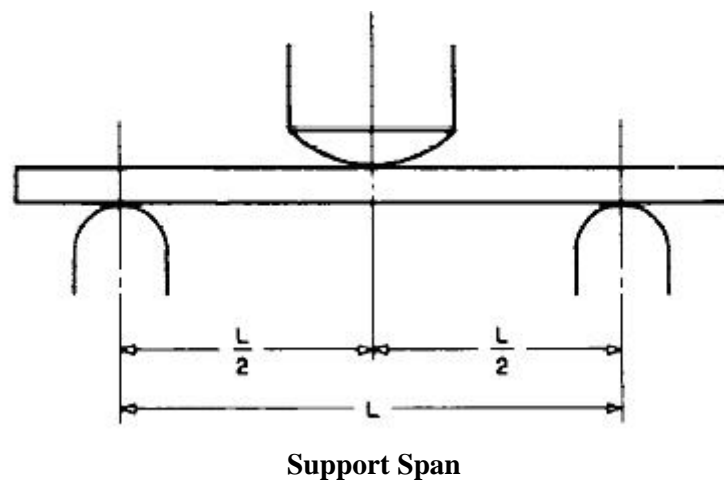


Figure 2.9 Three-point bending test [33].

2.6.1.3 Compressive Test

The compressive test is used to determine behavior of the materials under crushing loads as shown in Figure 2.10. The specimen is compressed and deformation at various loads is recorded. Compressive stress and strain are calculated and plotted as a stress-strain diagram which is used to determine elastic limit, proportional limit, yield point, yield strength and, for some materials, compressive strength. The compressive strength is a value of uniaxial compressive stress reached when the material fails completely. It is usually obtained experimentally by means of a compressive test. The apparatus used for this experiment is the same as that used in a tensile test. However, rather than applying a uniaxial tensile load, a uniaxial compressive load is applied [34-35].

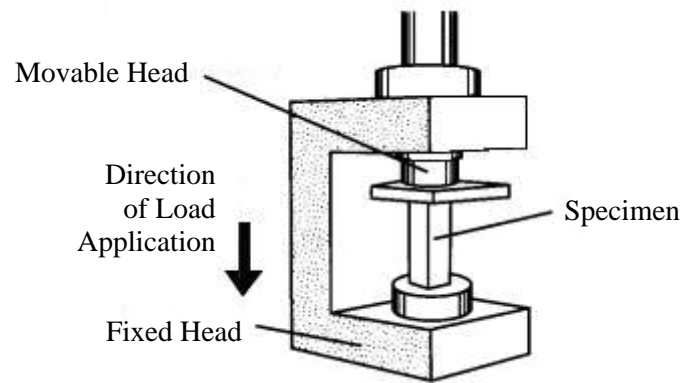


Figure 2.10 Compressive test [35].

2.6.1.4 Impact Test

The impact test is used to measure the resistance to failure of a material to a suddenly applied force such as collision, falling object or instantaneous blow. The test measures the impact energy, or the energy absorbed prior to fracture. Impact energy is a measure of the work done to fracture a test specimen. When the striker impacts the specimen, the specimen will absorb energy until it yields. At this point, the specimen will begin to undergo plastic deformation at the notch. The test specimen continues to absorb energy and work hardens at the plastic zone at the notch. When the specimen can absorb no more energy, fracture occurs. Brittle materials generally have lower impact strength, while those registering higher impact strengths tend to be tougher [36-37]. Figure 2.11 demonstrates the Izod impact machine.

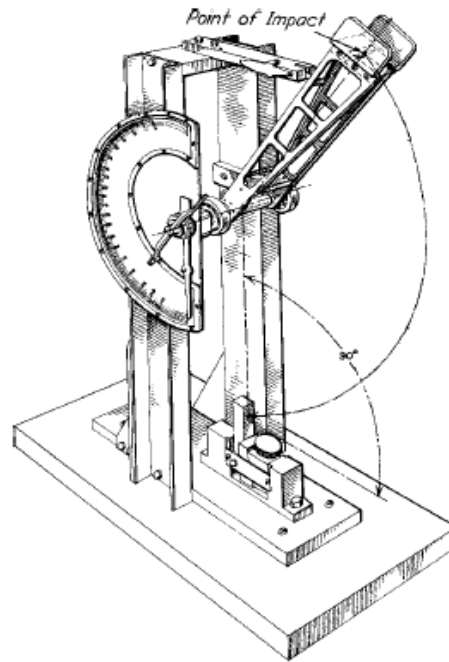


Figure 2.11 Izod impact machine [38].

2.6.2 Thermal Characterizations

2.6.2.1 Heat Deflection Temperature (HDT)

Heat deflection (or heat distortion) temperature (HDT) is the temperature which a sample bar of standard dimensions deflects by 0.25 mm (0.01 in.) under a standard flexural load of 455 kPa (66 psi) placed at its center. The sample is heated in an immersion bath at a rate of 2 °C/min. In the case of an amorphous polymer, HDT is slightly lower than the glass transition temperature (T_g) as determined by thermal techniques such as differential scanning calorimetry, while in the case of semi-crystalline polymers, HDT is more closely identified with melting crystalline temperature (T_m), as shown in Table 2.3. HDT is a useful indicator of the temperature limit above which polymer cannot be used for structure or load-supporting applications [39].

Table 2.3 Thermal-transition temperatures of commercial polymers [39].

Polymer	HDT* (°C)	T_g (°C)	T_m (°C)
Polyethylene	29 to 126	-120 to -125	137
Polypropylene	40 to 152	-10 to -18	176
Nylon-6,6	62 to 261	49	265
Poly(vinyl chloride)	60 to 76	87	Low crystallinity
Polycarbonate	39 to 148	150	Amorphous
Polystyrene	63 to 112	100	Amorphous
Polysulfone	146 to 273	190	Amorphous

*At 1.82 MPa (264 psi); HDT range indicates values reported for all commercial grades.

2.6.2.2 Dynamic Mechanical Analysis (DMA)

Dynamic mechanical analysis (DMA) is a technique used to study and characterize materials. It is most useful for observing the viscoelastic nature of polymers. Two methods are currently used. One is the decay of free oscillations and the other is forced oscillation. Free oscillation techniques involve applying a force to a sample and allowing it to oscillate after the force is removed. Forced oscillations involve the continued application of a force to the sample. An oscillating force is applied to a sample of material and the resulting displacement of the sample is measured. The test specimen is clamped between the movable and stationary fixtures, and then enclosed in the thermal chamber. Frequency, amplitude, and a temperature range appropriate for the material being tested are input. The elastic modulus (or storage modulus, G'), viscous modulus (or loss modulus, G'') and damping coefficient ($\tan D$) is determined as a function of temperature, frequency or time [40].

2.6.2.3 Thermogravimetric Analysis (TGA)

Thermogravimetric analysis (TGA) is a dynamic technique which the weight loss of a sample is measured continuously during a state where its temperature is increased at some constant rate. An alternative approach is to measure weight loss as a function of time at constant temperature. The main use of TGA in polymers application has been in studies of thermal decomposition, auto-oxidative, and stability. A TGA trace provides data of the weight loss at a thermal event occurs. A typical thermogram is illustrated in Figure 2.12 which comprises of a plot of change in weight (w) versus temperature (T). A small initial weight loss, such as that from w to w_0 , generally results from desorption of solvent. If it occurs near 100 °C, this is usually assumed to be loss of water. In the figure, extensive decomposition starts at T_1 with a weight loss w_0-w_1 . Between T_2 and T_3 another stable phase exists, and then further decomposition occurs [41].

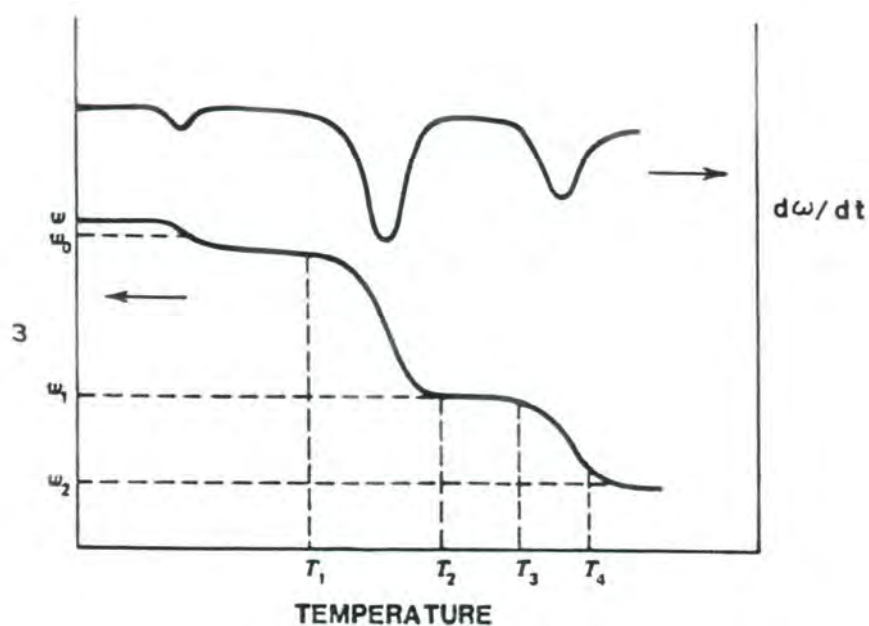


Figure 2.12 Typical TGA thermogram [41].

2.6.3 Morphology characterization

2.6.3.1 Scanning Electron Microscope (SEM)

The Scanning Electron Microscope (SEM) is a microscope that uses electrons rather than light to form an image. There are many advantages to using the SEM instead of a light microscope.

The SEM has a large depth of field, which allows a large amount of the sample to be in focus at one time. The SEM also produces images of high resolution, which means that closely spaced features can be examined at a high magnification. Preparation of the samples is relatively easy since most SEM on require the sample to be conductive. The combination of higher magnification, larger depth of focus, greater resolution and ease of sample observation makes the SEM one of the most heavily used instruments in research areas today.

A beam of electrons is generated in the electron gun, located at the top of the column, which is pictured to the left. This beam is attracted through the anode. Condensed by a condenser lens, and focused as a very fine point on the sample by the objective lens. The scan coils are energized (by varying the voltage produced by the scan generator) and create a magnetic field which deflects the beam back and forth in a controlled pattern. The varying voltage is also applied to the coils around the neck of the Cathode-ray tube (CRT) which produces a pattern of light deflected back and forth on the surface of the CRT. The pattern of deflection of the electron beam is the same as the pattern of deflection of the spot of light on the CRT.

The electron beam hits the sample producing secondary electron from the sample. These electrons are collected by a secondary detector of a backscatter detector converted to a voltage and amplified. The amplified voltage is applied to the grid of the CRT and causes the intensity of the spot of light to change. The image consists of thousands of spots of varying intensity on the face of a CRT the correspond to the topography of the sample [25].

CHAPTER III

LITERATURE REVIEWS

Fuad et al. [42] studied the effects of applying several types of coupling agents on the mechanical properties of rice husk ash (RHA)/polypropylene (PP) composites. The coupling agents studied include titanate (LICA 38), zirconate (NZ 44), silanes with and without peroxide group (PROSIL 2020 and PROSIL 9234) respectively. Polypropylene composites of 10-40 wt% RHA loadings were compounded by using a twin screw extruder. The experimental results indicated that without the use of any coupling agent, the flexural modulus increased with the RHA content while the tensile strength, elongation at break and the Izod impact strength decreased due to the poor interfacial adhesion between RHA and PP matrix. Silanes with peroxide group (PROSIL 2020) improved the tensile strength of the composites, while the impact properties were enhanced by the titanate coupling agent (LICA 38) and the silanes without peroxide group (PROSIL 9234). Only the zirconate coupling agent (NZ 44) increased the stiffness of the composites at maximum RHA loading. The SEM micrographs revealed an improvement in the adhesion between PP matrix and RHA when coupling agents were added.

Ismail et al. [21] studied the effects of a compatibilizer on the mechanical properties and the mass swell of natural rubber (NR)/linear low density polyethylene (LLDPE) blends (30:70 NR-to-LLDPE weight ratios) filled white rice husk ash (WRHA) at 15, 30 45 and 60 % by weight. Poly(propylene-ethylene-acrylic acid) (PPEAA) was used as the compatibilizer. WRHA filled NR/LLDPE blends with and without PPEAA were tested for their tensile properties, hardness and mass swell. The experimental results indicated that increasing WRHA loading in the NR/LLDPE blends resulted in a reduction of tensile strength, elongation at break and mass swell but the tensile modulus and the hardness were increased. The reductions in tensile strength and mass swell were due to poor interfacial bonding between the filler and the polymer matrix while the elongation at break of the NR/LLDPE blends decreased because WRHA hindered molecular mobility or deformability of the blends. At

equivalent WRHA loading, the presence of PPEAA increased the tensile strength, tensile modulus, hardness, and elongation at break but reduced the mass swell. The SEM micrographs showed improvement of interfacial bonding between the WRHA and the NR/LLDPE blends when PPEAA was added.

Ismail et al. [43] studied the effects of coupling agents on the properties of white rice husk ash (WRHA)-filled natural rubber (NR) compounds. The coupling agents used were a commercial silane coupling agent (Si69) and the multifunctional additive (EN444) which was a diamine salt of fatty acid. The WRHA was mixed with NR compounds at 10-50 phr by using a two-roll mill. The concentration of the coupling agents were varied at 0.5-3 phr. The experimental results indicated that the tensile modulus and the hardness increased with increasing WRHA loading while the elongation at break decreased due to the filler restricted the mobility of the macromolecular chains of the rubber. The tensile and tear strengths increased with increasing WRHA loading at 10 phr WRHA loading and then decreased. The reduction in strength may be due to the agglomeration of filler particles to form a domain that acts like a foreign body or simply the result of physical contact between adjacent aggregates. The incorporation of the multifunctional additive and silane coupling agent increased the cure rate and improved the tensile modulus, tensile strength, tear strength and hardness of WRHA-filled NR compounds. The SEM micrographs indicated that the coupling agents increased the rubber-WRHA interaction and improved the WRHA dispersion in the NR matrix.

Hassan et al. [44] studied the effects of impact modifiers on impact properties of rice husk ash (RHA) filled modified unplasticized PVC treated with titanate coupling agent (LICA38). Unplasticized PVC was filled with RHA at 10, 20 and 30 phr. The impact modifiers studied include acrylic impact modifier and chlorinated polyethylene (CPE) impact modifier which were added in unplasticized PVC at 2, 4, 6 and 8 phr. The mixtures were dry blended and rolled out as sheets on a two-roll mill before compression molded to prepare the composite specimens for impact testing. The experimental results indicated that the impact strength of the impact-modified PVC increased with increasing content of impact modifier due to it served to increase the toughness of the PVC matrix. However, acrylic impact modifier gave higher the impact strength compared to CPE impact modifier at 6 and 8 phr. For the content of

impact modifiers at 6 phr, the addition of RHA led to a reduction in the impact strength of the impact modified unplasticized PVC. The increase in brittleness of the composites was attributed to the weak interfacial adhesion between the RHA fillers and the PVC matrix. Titanate coupling agent (LICA38) was found to have enhanced the impact strength of the impact modified composites due to it improved the interfacial adhesion between the RHA fillers and the PVC matrix.

Yang et al. [45] studied the possibility of using lignocellulosic materials as reinforcing fillers in thermoplastic composite. They used polypropylene as the matrix and rice-husk flour as the reinforcing filler at 10, 20, 30 and 40 % by weight. The tensile tests were performed at crosshead speeds of 2, 10, 100, 500 and 1500 mm/min, and temperatures of -30, 0, 20, 50, 80 and 110 °C. The experimental results indicated that the tensile strengths of the composites decreased slightly while the tensile modulus improved as the filler loading and crosshead speed increased. Notched and unnotched Izod impact strengths decreased with increasing filler loading. The composite became brittle at higher crosshead speed, and showed plastic deformation with increasing test temperature.

Premalal et al. [46] compared the mechanical properties of rice husk powder (RHP)-filled polypropylene (PP) composites with talc-filled polypropylene composites. PP was filled with ground talc and RHP separately 15, 30, 45 and 60 phr (per 100 part of polymer). They investigated the mechanical properties of the composites with reference to the filler type and the filler loading. The experimental results indicated that the Young's modulus and the flexural modulus increased while the yield strength and the elongation at break decreased with increasing filler loading for both types of composites. The PP/RHP composites exhibited lower yield strength, Young's modulus, flexural modulus, and higher elongation at break than the PP/talc composites. The SEM photographs indicated poorer interfacial adhesion and dispersion of the PP/RHP composites compared with those seen in the PP/talc composites.

Garcia et al. [47] studied the effects of rice husk contents and particle sizes on the tensile properties of recycled rubber. The used recycle rubber which was wastes from tires without steel or other type of fibers had average particle size of 0.3

mm. They mixed rice husk (particle sizes of 0.75, 0.37 and lower than 0.1 mm) with recycled rubber at 0, 5, 10, 15, 20 and 25 % by weight in a hot plate press with pressure of 2 MPa and temperature of 180 °C in order to avoid the thermal decomposition of rice husk. The experimental results indicated that an increment in rice husk content enhanced the tensile modulus while decreases the tensile strength and the strain at break. This was due to the higher stiffness of the rice husk produced an increase in the stiffness of the composites at low strains. Contrarily, at high strains, bonds between the rice husk and the rubber matrix became weak and debonding resulted in interfacial failure, the ultimate strength and strain at break were decreased. Compared with the rubber composites with different particle sizes of rice husk, rice husk particles, which had an average size (0.37 mm) similar to that of rubber powder (0.3 mm), had the highest tensile modulus and strength because of more mixable in like particle sizes of rice husk and rubber powder. The SEM micrographs showed a more uniform distribution of rice husk particles within the rubber matrix as the particle sizes decreased and the low interfacial bonding between the rice husk and the matrix.

Jangchud et al. [48] studied the effects of natural rubber fiber (NRF) content and loading of plasticizer (dioctyl phthalate, (DOP)) on the mechanical properties of untreated NRF-poly(vinyl chloride) (PVC) composites. Formulas of the PVC composites contained PVC, natural rubber fibers (0-50 phr), DOP (5-20 phr) and other additives were compounded in a high-speed mixer then melt-blended by using a single-screw extruder and shaped into test specimens by a compression molding machine. The experimental results indicated that an increase in the NRF content led to higher tensile strength, modulus at 3% strain, flexural strength, flexural modulus and impact strength. The hardness of the composites increased with increasing NRF content. Very high fiber loading was limited due to difficulty in mixing high volume of fibers. Insufficient fiber dispersion was viewed as defects in the composites resulting in deterioration of the mechanical properties. By increasing the DOP plasticizer loading, the mechanical properties in terms of tensile strength, modulus at 3% strain, flexural strength, flexural modulus and hardness were decreased due to plasticization effect of the DOP. As expected, the impact strength was increased with an increase in the DOP which softened the PVC.

Stark et al. [49] studied the effect of particle size on the properties of wood-flour (WF) filled polypropylene (PP) composites. Ponderosa pine (*Pinus ponderosa*) was used as a filler. Eight wood flours included four screened wood flours (35, 70, 120 and 235 meshes), and four commercially available wood flours (20, 40, 80 and 120 meshes). Each particle size of WF was blended with PP at 40 % by weight in a twin-screw extruder and injected to prepare the WF/PP specimens. The experimental results indicated that specific gravity of the WF/PP composites was independent of WF particle sizes. As WF particle size increased, the volume of unfilled regions within the polymer increased, resulting in greater flow mobility for the polymer and higher melt index values. The flexural and tensile modulus and strength, and percentage of tensile elongation increased with increasing WF particle sizes. Moreover, the notched impact strength increased with the larger WF particles because the crack propagated at the weaker wood-polymer interface and traveled around the wood particles. Since the fracture surface area increased with increasing particle size, more energy is required to fracture the impact specimen with larger particles. However, unnotched impact strength decreased with greater WF particles due to the larger particle sizes provide higher stress concentrations where a crack can be initiated more easily.

Ismail et al. [50] studied the effects of filler content and size on properties of epoxidized natural rubber (ENR) composites. The filler used was oil palm wood flour (OPWF) which had three different sizes (75-180, 180-270 and 270-500 μm) were filled and unfilled with ENR at 0, 15, 30, 40 and 50 phr. The experimental results indicated that there was a cure enhancement of OPWF-ENR composites with increasing filler content. The larger particles size of OPWF showed shorter cure and scorch times than the small particles size. The maximum torque increased with increasing fiber content and OPWF with smallest particles size showed the highest torque values. Addition of OPWF in ENR compounds increased tear strength, tensile modulus and hardness but decreased tensile strength and elongation at break of the composites. The strength of the composites decreased due to the inability of the filler to support stresses transferred from the polymer matrix. The smaller particle size of OPWF gave better the mechanical properties than the larger particle sizes because the smaller OPWF particle was better dispersed in the polymer matrix than the larger

OPWF particle. The SEM micrographs showed the occurrences of fiber bundles pull-out in the OPWF-ENR composite. As the filler content increased the dispersion and wettability of the composites worsen and consequently the strength of the composites decreased steadily.

Kim et al. [51] studied the effects of a coupling agent on the structure and the properties of stretched PP/wood-fiber (WF) 30 % by weight composites-based artificial wood. The WF used was softwood (pine). The coupling agent used was maleated graft-PP (MAPP) at 1, 3 and 5 % by weight. The mixtures were mixed by using twin-screw extruder. The experimental results indicated that the artificial wood adopted a texture similar to that of natural wood. The number of voids for the composites with MAPP decreased and the voids became shorter compared with the composites without MAPP. The MAPP improved the interfacial adhesion between the WF and the PP matrix and the dispersion of WF in the polymer matrix. It increased the tensile strength of the PP/WF composites. However, when MAPP was added, the density reduction became smaller and more difficult due to the enhanced adhesion between the WF and the PP matrix. As the content of MAPP increased, the tensile strength and the modulus increased while the elongation at break decreased steadily because of enhanced interfacial bonding.

Suarez et al. [52] studied tensile fracture surfaces of polypropylene (PP)/sawdust composites. The matrix was polypropylene (PP) with maleated polypropylene (MAPP) (0, 2, 5, 10, 20 and 40 % by weight of the matrix). They mixed the sawdust, which was coated with 22.4 % by weight of MAPP, with the matrix at 20 % by weight. The mixtures were blended and then molded sheets to prepare the PP/sawdust composite specimens for tension testing. The experimental results indicated that the tensile strength of the PP composites was lower than that of the PP/MAPP composites due to a weak interfacial region reduced the efficiency of stress transfer from the matrix to the reinforcement component. The composites with a MAPP content lower than 20 % by weight had smaller the tensile properties. The composites with higher concentrations of MAPP showed an increase in the tensile strength with an ultimate elongation similar to that of the composite without MAPP. At 40 % by weight of MAPP, the PP/sawdust composite had the highest tensile

strength and an ultimate elongation. The SEM micrographs showed that the addition of MAPP to PP enhanced the interfacial adhesion between sawdust and PP matrix.

Zheng et al. [53] studied the interface modification of bagasse fibre (BF) and the mechanical properties of BF/poly(vinyl chloride) (PVC) composites. The BF was mixed with PVC compounds at 15, 25 and 35 % by weight by using a two roll mill. The concentration of benzoic acid (modifier) was varied at 3, 5, and 10 % by weight. The experimental results indicated that the tensile strength clearly increased as the content of BF and the content of the modifier increased due to the improvement of the interfacial adhesion made the fibre act as an agent of reinforcement in PVC matrix. The impact strength and the elongation at break of the composites decreased as the content of BF increased but benzoic acid did not significant change. The decrease of the impact strength and the elongation at break might be due to the higher brittleness introduced by blending BF with the PVC matrix. The tensile modulus increased as the content of the BF increased. The treatment with benzoic acid improved the modulus of the composite when it increased up to 5 % by weight and then decreased. The SEM photographs indicated that benzoic acid effectively increased the adhesion and significantly improved the dispersion of BF in the PVC matrix.

Zhu et al. [54] studied the effects of grafted polymer on the morphology and property of nanosilica/PVC composites. Silica nanoparticles were pre-treated with a silane coupling agent (γ -methacryloxypropyl trimethoxy silane, MPS) and then treated with grafted polymer to prepare poly(methyl methacrylate)-grafted-nanosilica (PMMA-g-silica) and a copolymer of styrene, n-butyl acrylate and acrylic acid-grafted-nanosilica (PSBA-g-silica) hybrid nanoparticles. Hybrid nanoparticles and untreated nanosilicas were mixed with the PVC compound at 2.5 % by weight, blended on a two-roll mill and hot pressed to prepare the composite specimens. The experimental results indicated that the tensile strength and the elongation to break of the hybrid nanocomposites improved significantly in comparison with that of untreated nanosilica/PVC composites. The storage modulus and the T_g of PMMA-g-silica/PVC nanocomposite were higher than that of the unfilled PVC, however, the storage modulus and the T_g of PSBA-g-silica/PVC nanocomposite were lower than that of unfilled PVC. This was because the entanglement of the rigid grafted PMMA with PVC restrains the motion of PVC chains while PSBA grafted on nanosilica

favors the chain motion of PVC. Morphology study of PVC nanocomposites revealed that both PMMA- and PSBA-grafted-silica had an adhesive interface between the silica and PVC. The dispersion of nanosilica improves greatly due to the steric hindrance of the grafted polymer.

CHAPTER IV

EXPERIMENTS

4.1 Materials

PVC compounded powder (K66) was used as polymer matrix. Its melting temperature ranges between 170-190 °C with a density of 1.4 g/cm³ at room temperature. The filler was white rice husk ash which was obtained as waste from small electricity generating plant where rice husk was burnt at 800-900 °C. Figure 4.1 shows raw materials used in this research.

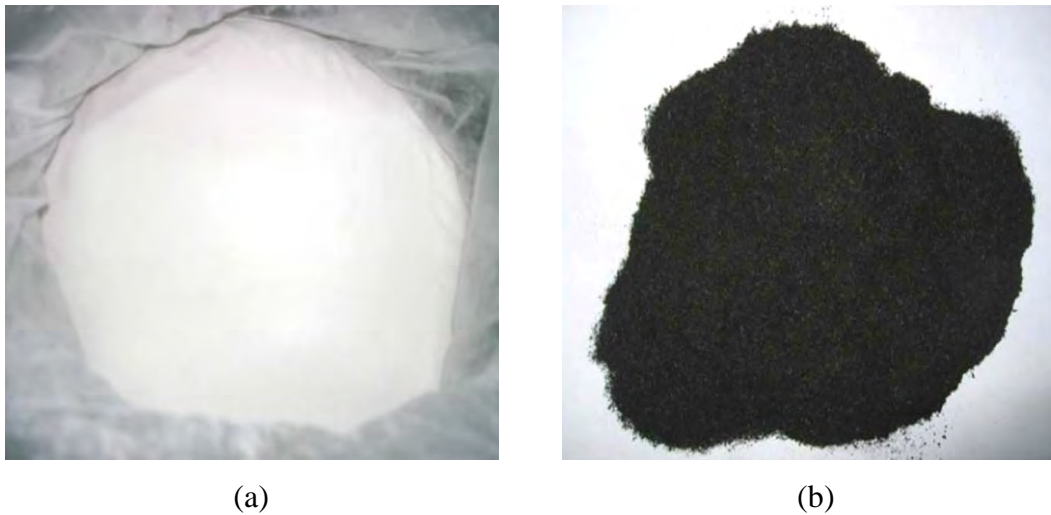


Figure 4.1 Raw materials: (a) PVC compound and (b) Rice husk ash.

4.2 Experimental Procedure

4.2.1 Preparation of Rice Husk Ash (RHA)

The RHA used in this research is white rice husk ash (WRHA). It was selected for this work because of its extremely low cost and availability in Thailand. The RHA was grinded by using a vibration ball mill as shown in Figure 4.2(a) and sieved to the particle sizes of 45, 75, 106, 180 and 250 μm . Each size of grinded RHA was dried in an oven at 105 $^{\circ}\text{C}$ for 24 hours before use. Figure 4.2(b) show a sieve analyzer.

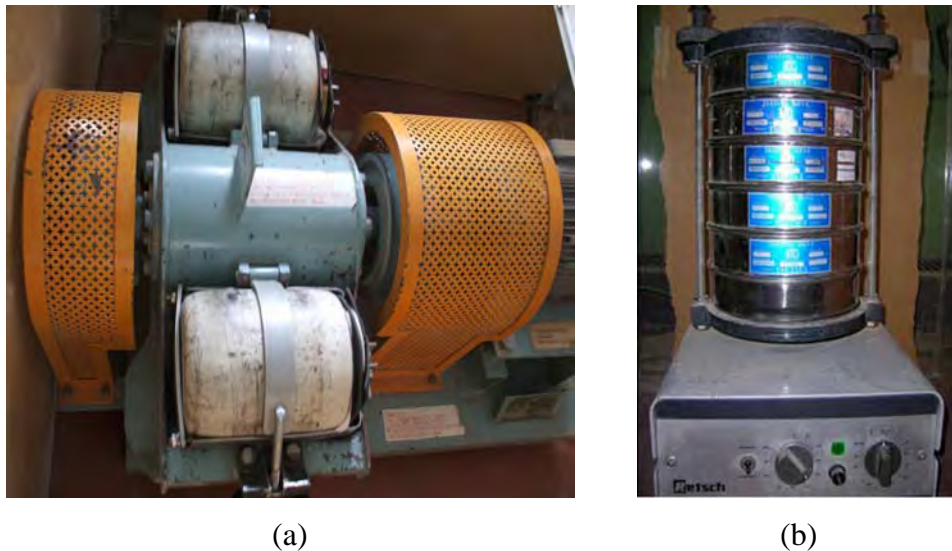


Figure 4.2 Grinding and sieving: (a) Vibration ball mill and (b) Sieve analyzer.

4.2.2 Processing of the PVC/RHA Composites

RHA of each size was mixed with PVC compound at 20, 40, 60 and 80 phr in a two-step high speed mixer (Plasmec model TRL), as shown in Figure 4.3(a), at the speed of 1300-1500 rpm. The temperature of the hot and the cold mixer were 110 $^{\circ}\text{C}$ and 40 $^{\circ}\text{C}$ respectively. The blends were compressed by using a hydraulic press (LAB TECH Engineering Company Ltd. model LP 50), as shown in Figure 4.3(b), at 190 $^{\circ}\text{C}$ and pressure of 70 kg/cm^2 for 5 minutes to prepare the standard specimens for

several mechanical tests according to American Society for Testing and Materials (ASTM). Profiles of PVC/RHA composites were extruded by using an industrial scale conical counter rotating twin screw extruder. Figure 4.3(c) demonstrates the industrial scale twin screw extruder used in the present study.



(a)



(b)



(c)

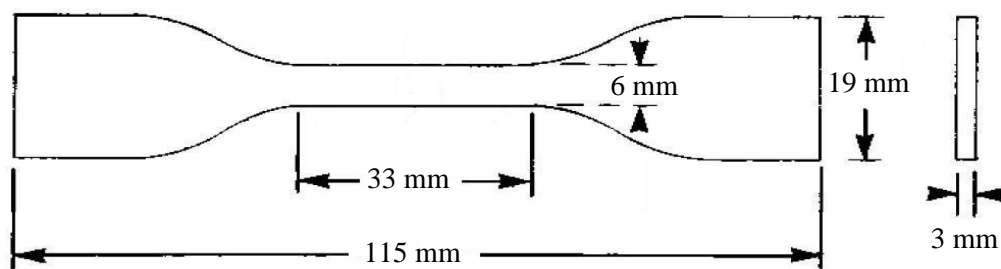
Figure 4.3 Blending and processing: (a) Dry blender, (b) Hydraulic press and (c) Industrial scale twin screw extruder.

4.3 Testing and Characterizations

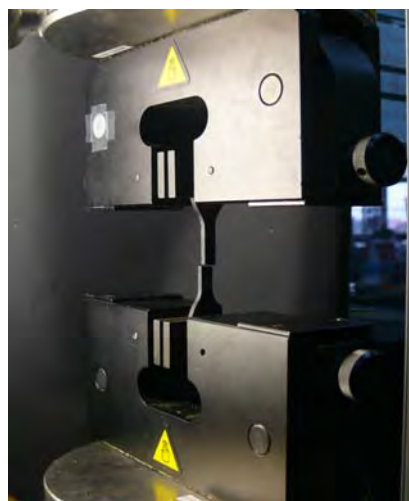
4.3.1 Mechanical Properties

4.3.1.1 Tensile Test

The tensile modulus and the tensile strength of the PVC/RHA composites were obtained by using a universal testing machine (Instron Instrument, model 5567) according to ASTM D 638 – 03 [55]. The test specimens are dumbbell shape with a uniform thickness as shown in Figure 4.4(a). The test was performed at a crosshead speed of 1.2 mm/min and a gage length of 50 mm. The average tensile properties reported were values taken from five specimens of identical formulation. Figure 4.4(b) shows the tensile properties test.



(a)



(b)

Figure 4.4 Tensile properties test: (a) Tensile test specimen and (b) Tensile test.

4.3.1.2 Flexural Test

The flexural modulus and the flexural strength of the PVC/RHA composites were also measured by using a universal testing machine (Instron Instrument, model 5567) using the procedure according to ASTM D 790 – 03 [33]. The dimension of the specimens was 12.7 mm × 96 mm × 3 mm as shown in Figure 4.5(a). Three-point bending test was performed at room temperature at a crosshead speed of 1.2 mm/min with the support span of 76 mm, as exhibited in Figure 4.5(b). The flexural properties estimated were average obtained from five specimens of each formulation.

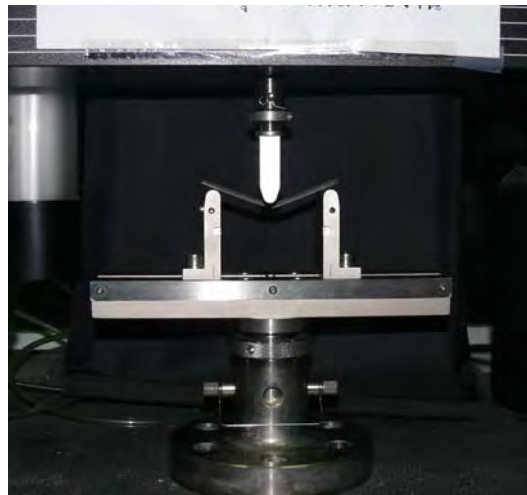
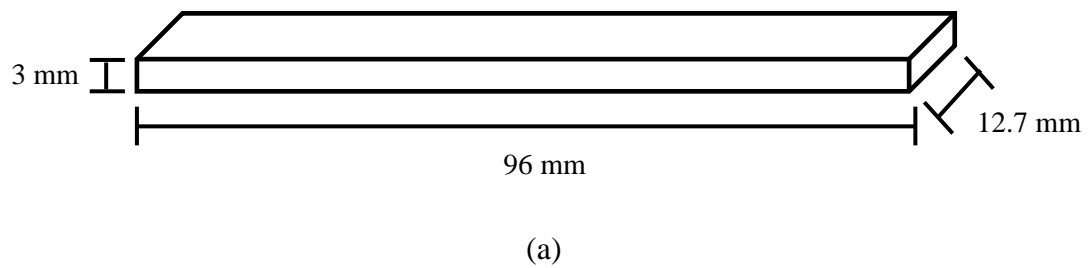


Figure 4.5 Flexural properties test: (a) Flexural test specimen and (b) Flexural test.

4.3.1.3 Compressive Test

The compressive modulus and the compressive strength of the composite specimens were obtained also by using a universal testing machine (Instron Instrument, model 5567) according to ASTM D 695 – 02 [56]. They were tested using a crosshead speed of 1.2 mm/min at room temperature. The dimensions of the specimens were 12.7 mm × 12.7 mm × 3 mm as shown in Figure 4.6(a). Figure 4.6(b) indicates the compressive test specimen placed between two parallel compressive plates. The average compressive properties reported were values taken from five specimens of each formulation.

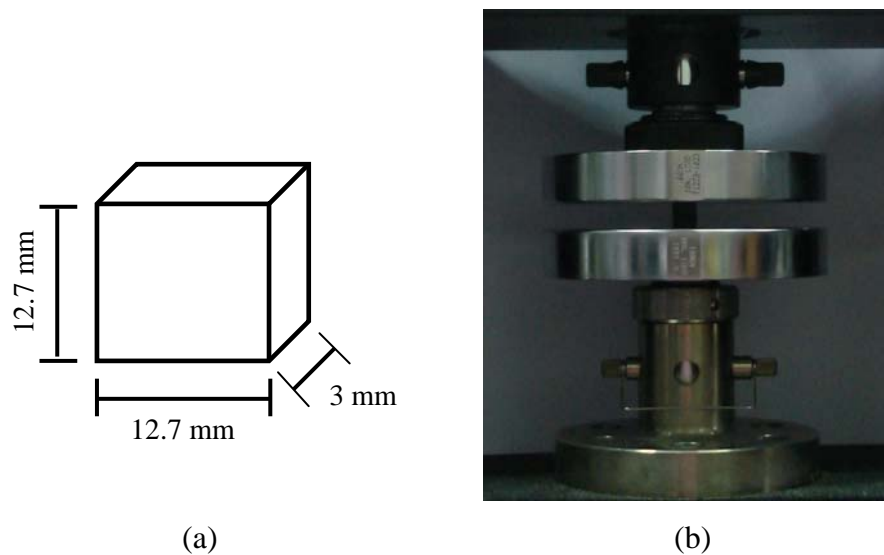
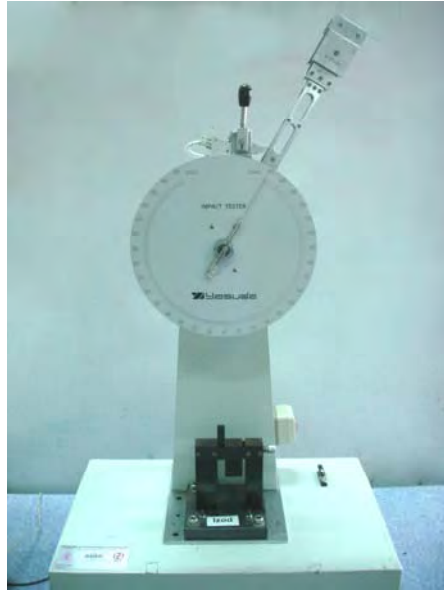


Figure 4.6 Compressive properties test: (a) Compressive test specimen and (b) Compressive test.

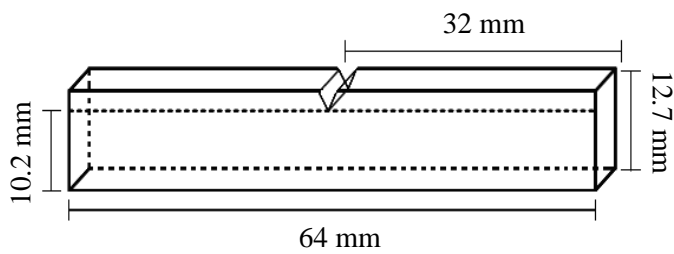
4.3.1.4 Notched Izod Impact Test

The notched Izod impact strength of the PVC/RHA composite specimens was determined by using an Izod impact tester (Yasuda Impact Tester), as shown in Figure 4.7(a), according to ASTM D 256 – 06 [38]. The dimensions of the specimens were 64 mm × 12.7 mm × 6 mm with 45° notching angle as shown in Figure 4.7(b). Each specimen was placed so that the notch faced the impact pendulum

as shown in Figure 4.7(c). The average impact energy obtained from five specimens of each formulation was reported.



(a)



(b)



(c)

Figure 4.7 Notched Izod impact properties test: (a) Izod impact tester, (b) and (c) Notched Izod impact test specimen.

4.3.2 Thermal Properties

4.3.2.1 Heat Deflection Temperature (HDT)

The heat deflection temperature (HDT) was investigated by following ASTM D 648 – 06 [57]. The dimensions of the specimens were 120 mm x 12.7 mm x 3 mm. It was loaded under a three-point bending mode. The load used for this test was 0.455 MPa and the temperature was increased at 2 °C/min until the specimen deflects 0.25 mm. Figure 4.8 shows the heat deflection temperature test. The HDT reported was average value obtained from three specimens of each formulation.

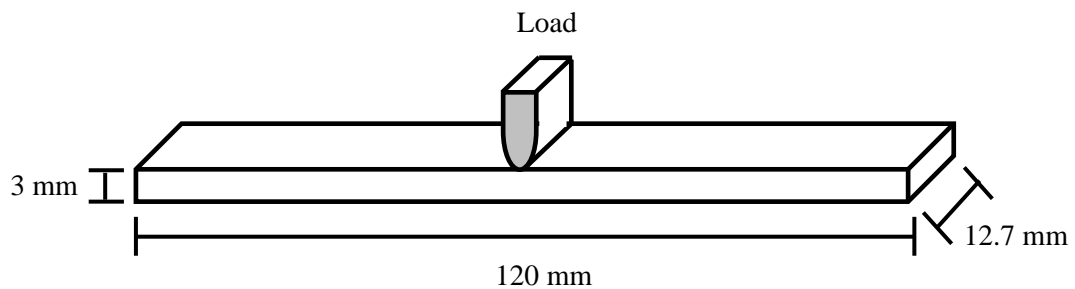


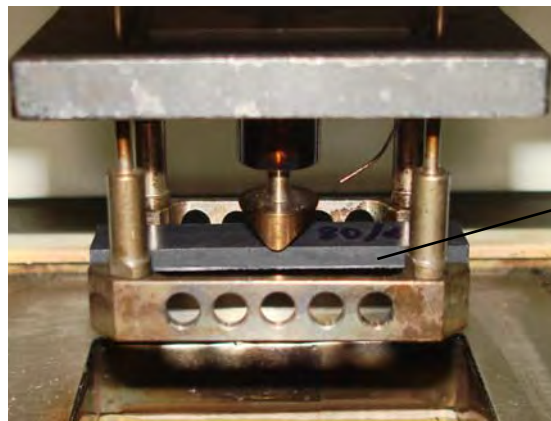
Figure 4.8 Heat deflection temperature test specimen.

4.3.2.2 Dynamic Mechanical Properties

Figure 4.9(a) shows the dynamic mechanical analyzer (DMA) (NETZSCH model DMA242) which was used to investigate the dynamic mechanical properties of the PVC/RHA composites. The dimensions of specimens were 10 mm × 55 mm × 3 mm as shown in Figure 4.9(b). The test was performed in a 3-point bending mode with a heating rate of 2 °C/min from room temperature to 130 °C under nitrogen atmosphere. The storage modulus (G'), loss modulus (G'') and loss tangent or damping curve ($\tan \delta$) were obtained. The glass transition temperature (T_g) was taken as the temperature corresponding to the maximum on the loss tangent curve in the DMA thermogram.



(a)



(b)

Figure 4.9 Dynamic mechanical analysis: (a) Dynamic mechanical analyzer and (b) Dynamic mechanical test specimen.

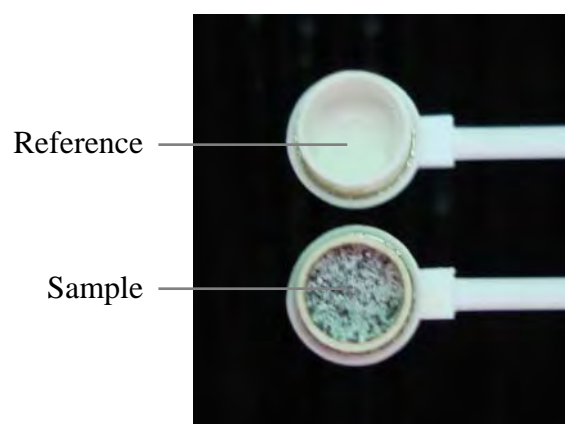
4.3.2.3 Thermogravimetric Analysis (TGA)

The thermal behaviors of each PVC/RHA composite in terms of the decomposition temperature (T_d) and the char yield of the composites were determined by using a thermogravimetric analyzer (TA instruments, SDT Q600) as shown in Figure 4.10(a). About 10 mg of the PVC/RHA composite powder was heated from 30 °C to 900 °C at a heating rate of 10 °C/min under nitrogen atmosphere. Figure 4.10(b) demonstrates the PVC/RHA composite sample. The gas flow rate of the purged nitrogen was 100 ml/min. The weight loss of each composite was

measured as a function of temperature. The T_d ranges and the char yield of all the PVC/RHA composites in this work were recorded.



(a)



(b)

Figure 4.10 Thermogravimetric analysis: (a) Thermogravimetric analyzer and (b) The PVC/RHA composite sample.

4.3.3 Physical Characterizations

4.3.3.1 Density

Density determination was performed by applying Archimedes' principle which stated that every solid body immersed in a fluid apparently lost weight by an amount equaled to that of the fluid it displaced. The PVC/RHA composite specimens were weighed in air and then they were immersed and weighed again in water. The density can be calculated from the two weights as shown in Equation (4.1).

$$\rho = \left[\frac{A}{(A - B)} \right] \times \rho_0 \quad (4.1)$$

where ρ = density of the composite, g/cm³
 A = weight of the composite in air, g
 B = weight of the composite in the liquid, g
 ρ_0 = density of water at the given temperature, g/cm³ (ρ_0 is temperature dependent)

The average density of the PVC/RHA composites reported in this research were average values obtained from three density measurements per each formulation of the composites. Figure 4.11 demonstrates density measurement equipment.

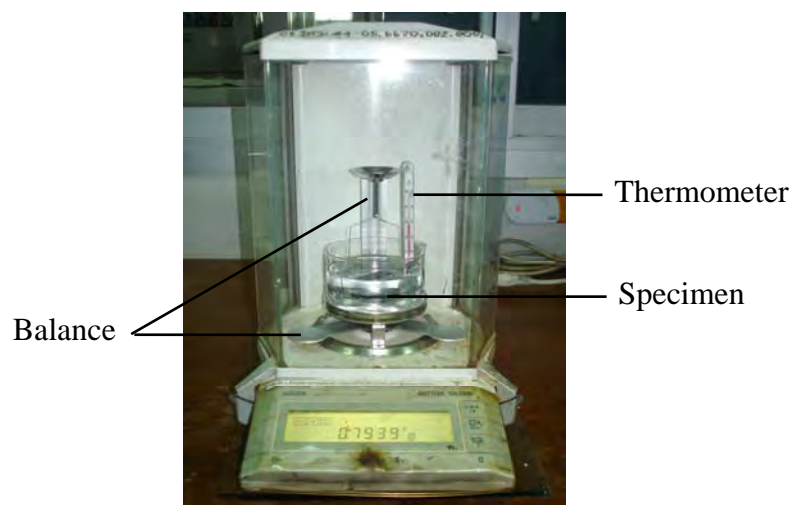
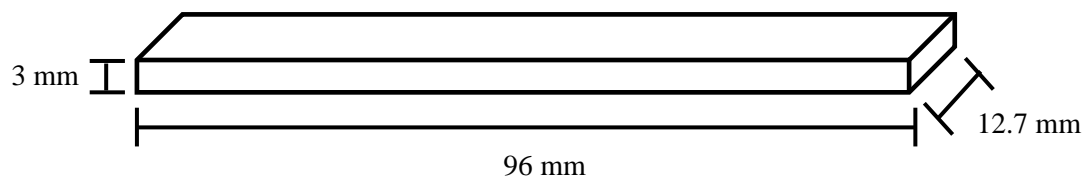


Figure 4.11 Density measurement equipment.

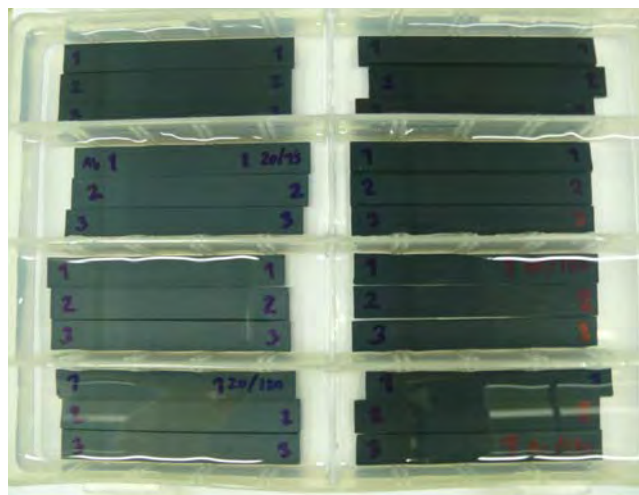
4.3.3.2 Water Absorption

The water absorption according to ASTM D 570 – 98 [58], which was used to measure the absorption of water by test was performed plastics when immersed in distilled water at room temperature as shown in Figure 4.12. The dimensions of the PVC/RHA specimen were 12.7 mm × 96 mm × 3 mm. Each specimen of the PVC/RHA composites was firstly weighed everyday for a week. Then they were weighed every other day for two weeks. Finally the composites were weighed every seventh day over the soaked period of two months. The water absorption, expressed as an increase in weight percent, can be calculated by using Equation (4.2). The water absorption averaged from measurements made on three specimens of each formulation was reported.

$$\text{Percent water absorption (\%)} = \left[\frac{\text{Wet weight} - \text{Dry weight}}{\text{Dry weight}} \right] \times 100 \quad (4.2)$$



(a)



(b)

Figure 4.12 Water absorption test.

4.3.3.3 Outdoor Weathering Test

The outdoor weathering test was performed according to ASTM D 1435 [59]. The PVC/RHA composite specimens have no specified size. They were mounted on a plate and placed outdoor as shown in Figure 4.13. The color changes of the composite specimens after an exposure of 30 days were observed.

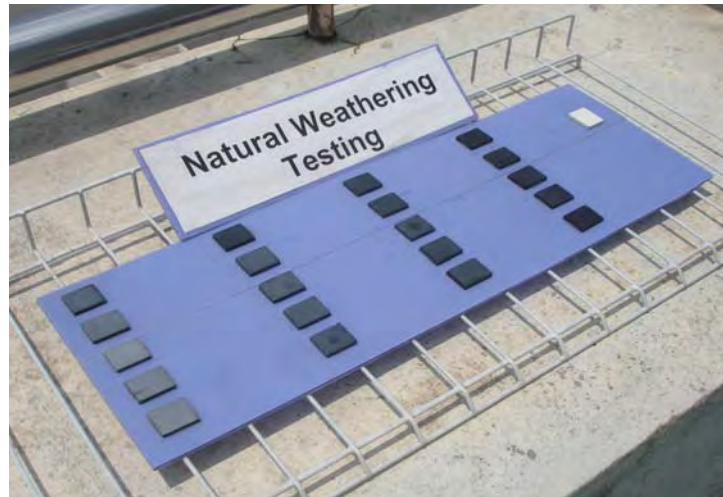


Figure 4.13 Outdoor weathering test.

4.3.3.4 Microscopic Observation

Samples of the PVC/RHA composites were cracked cryogenically and coated with a thin film of gold. The fracture surfaces of the PVC/RHA composites were studied by using a scanning electron microscope (SEM) (JEOL model JSM-5410 LV) at an acceleration voltage of 15 kV. Figure 4.14 shows a scanning electron microscope. The SEM micrographs were used to investigate the dispersion and the interfacial adhesion between the RHA filler and the PVC matrix.



Figure 4.14 Scanning electron microscope (SEM).

CHAPTER V

RESULTS AND DISCUSSION

The effects of rice husk ash (RHA) contents and RHA particle sizes on the mechanical, thermal, physical, and morphological properties were studied and presented in this chapter.

5.1 Mechanical Properties of the PVC/RHA Composites

5.1.1 Tensile Properties

The tensile modulus of the PVC/RHA composites is shown in Figure 5.1. The tensile modulus of the PVC compound was about 1.72 GPa which was lower than those of all the PVC/RHA composites. The tensile modulus of the composites increased with RHA contents. Compared with the PVC compound, the tensile modulus of the PVC/RHA composites with 20, 40, 60 and 80 phr of RHA were raised to 21.6%, 34.1%, 49.3% and 54% respectively. This increment of the tensile modulus is in agreement with Ismail et al. [43] who studied the mechanical properties of white rice husk ash (WRHA) filled natural rubber (NR) compounds. They found that the tensile modulus of the NR/WRHA composites increased with WRHA content and increased to approximately 26 % at 50 phr compared with the NR compounds. This is due to the inclusion of the rigid RHA particles which consist of high silica content. Therefore, the composites had more rigidity when RHA was added.

Figure 5.2 shows the tensile strength of the PVC compound and the PVC/RHA composites. The tensile strength of the PVC compound was 39 MPa, which was higher than those of the PVC/RHA composites. The tensile strength of the composites decreased with increasing RHA contents. This may be due to the agglomeration of the RHA filler in the PVC matrix. In the same way, the filler cannot support stresses which are transferred from the polymer matrix due to poor interfacial

adhesions between the PVC matrix and the RHA particles. Figure 5.5 shows the SEM micrographs which were found the poor interfacial adhesions between the PVC matrix and the RHA particles of the PVC/RHA composites.

In the case of RHA particles sizes, the tensile modulus and the tensile strength of the PVC/RHA composites with fine RHA particles were not significantly different from those of the composites with large RHA particles.

The tensile modulus of the PVC/RHA composites with 20 to 80 phr which was about 2.04 - 2.65 GPa was in range of the tensile modulus of commercial PVC/wood composites (between 1.97 - 5.80 GPa) [60-62]. Moreover, the tensile strength of the PVC/RHA composites with 20 to 60 phr was in range of the tensile strength of commercial PVC/wood composites (between 25.1 - 48.3 MPa) [60-62] while the tensile strength of the PVC/RHA composites with 80 phr was lower than those of commercial PVC/wood composites. This result indicated that the PVC/RHA composites with 20 to 60 phr can be used to substitute natural wood in application of wood plastic composites under tension load. However, the tensile strength of natural wood was between 46.5 - 120.7 MPa [63].

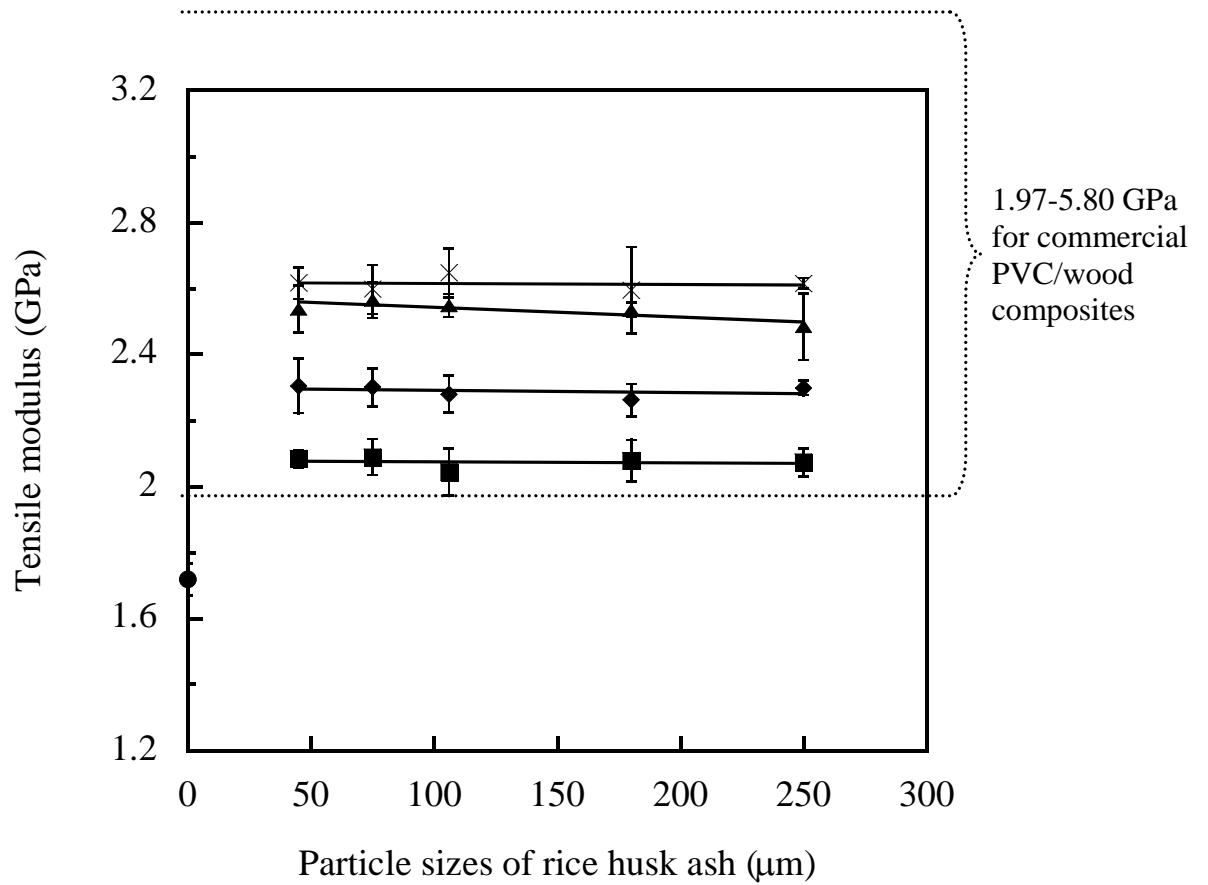


Figure 5.1 RHA contents on the tensile modulus of the PVC/RHA composites with various at 0 phr (●), 20 phr (■), 40 phr (◆), 60 phr (▲) and 80 phr (×) and different RHA particle sizes.

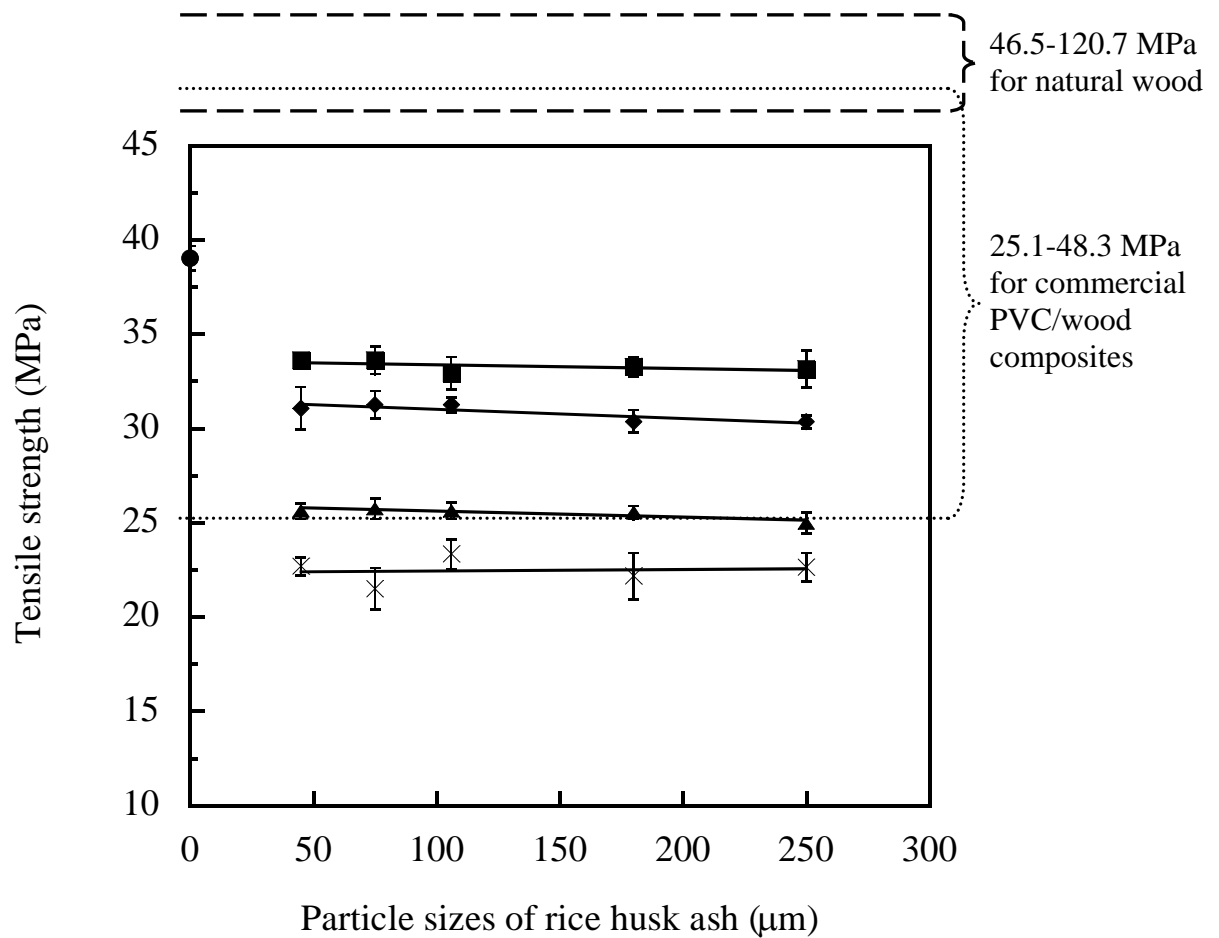


Figure 5.2 RHA contents on the tensile strength of the PVC/RHA composites with various at 0 phr (●), 20 phr (■), 40 phr (◆), 60 phr (▲) and 80 phr (×) and different RHA particle sizes.

5.1.2 Flexural Properties

Figure 5.3 exhibits the modulus of the PVC compound and the PVC/RHA composites under flexural modes. Similar to the tensile modulus, the flexural modulus of the PVC/RHA composites increased as RHA content increased. The flexural modulus of PVC compound was 2.11 GPa. In comparison with the PVC compound, the flexural modulus of the PVC/RHA composites was increased by approximately 21.6%, 28.7%, 48.4%, and 71.7% when the composites were filled with RHA by 20, 40, 60, and 80 phr respectively. This is due to the incorporation of the rigid RHA, which rich in silica, so the composites had more stiffness.

The flexural strength of the PVC/RHA composites is shown in Figure 5.4. The flexural strength of the composites decreased with increasing RHA contents. The flexural strength of the PVC compound was 44.07 MPa which was higher than those of the PVC/RHA composites. The flexural strength of the composites at various RHA contents (from 20 to 80 phr) decreased by approximately 9.8 to 16.5% compared with the PVC compound. This result can be explained from the SEM micrographs as shown in Figure 5.5. They indicate that the poor interfacial bonding between the PVC matrix and the RHA particles caused the decrement of the flexural strength.

The sizes of RHA particles had no significant effects on the flexural modulus and the flexural strength of the PVC/RHA composites.

Compared with commercial PVC/wood composites, the flexural modulus of the PVC/RHA composites with 20 to 80 phr which was about 2.50 - 3.63 GPa was in range of the flexural modulus of commercial PVC/wood composites (between 2.2 - 5.1 GPa) [60-62] but lower than those of natural wood (between 5.2 - 13.7 GPa) [63]. In addition, the flexural strength of the PVC/RHA composites with 20 to 80 phr was lower than those of commercial PVC/wood composites (between 41.3 - 66.0 MPa) [60-62,64] and natural wood (between 45 - 139 MPa) [63]. This result denoted that the PVC/RHA composites did not become to be used as WPCs under bending load.

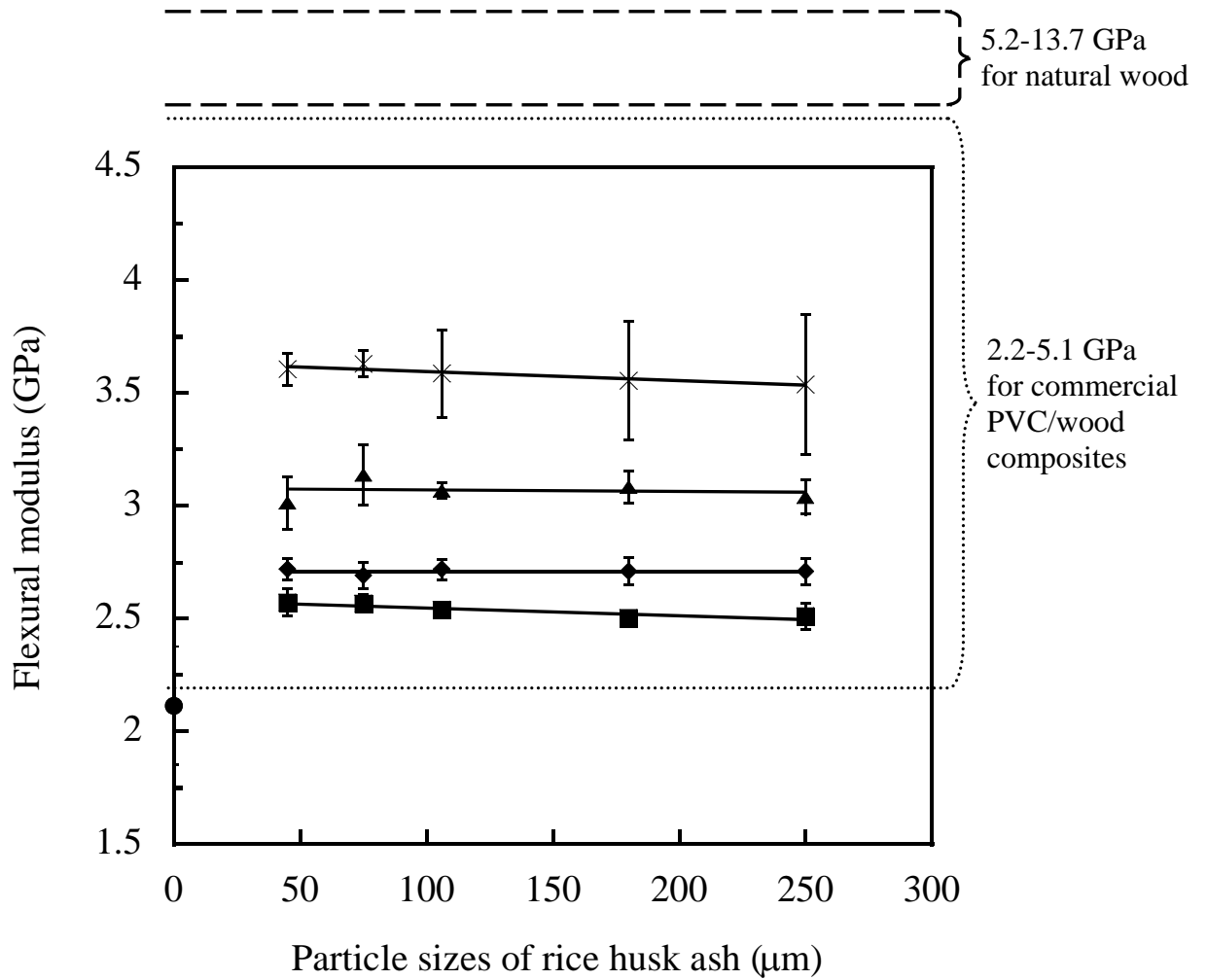


Figure 5.3 RHA contents on the flexural modulus of the PVC/RHA composites with various at 0 phr (●), 20 phr (■), 40 phr (◆), 60 phr (▲) and 80 phr (×) and different RHA particle sizes.

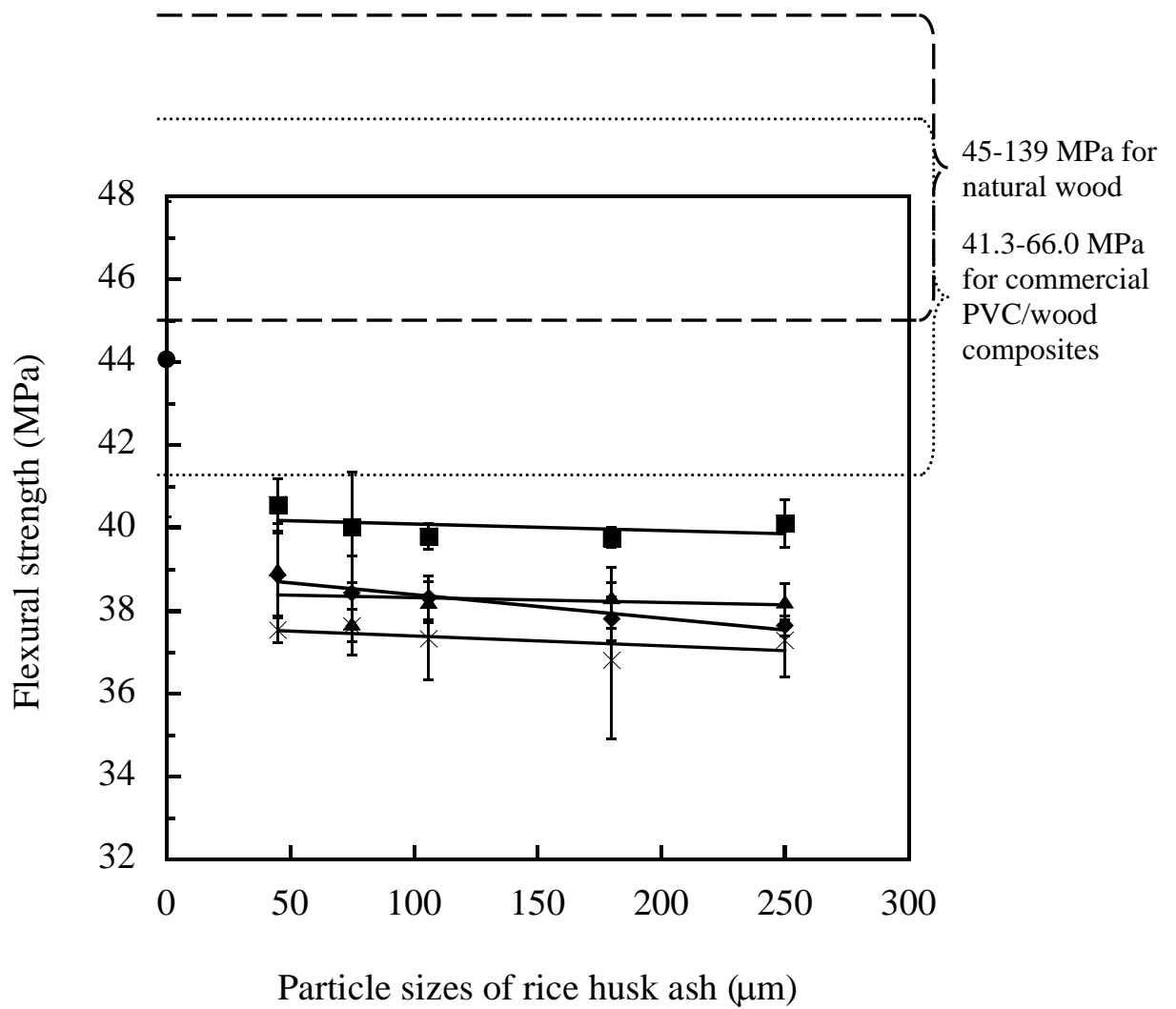


Figure 5.4 RHA contents on the flexural strength of the PVC/RHA composites with various at 0 phr (●), 20 phr (■), 40 phr (◆), 60 phr (▲) and 80 phr (×) and different RHA particle sizes.

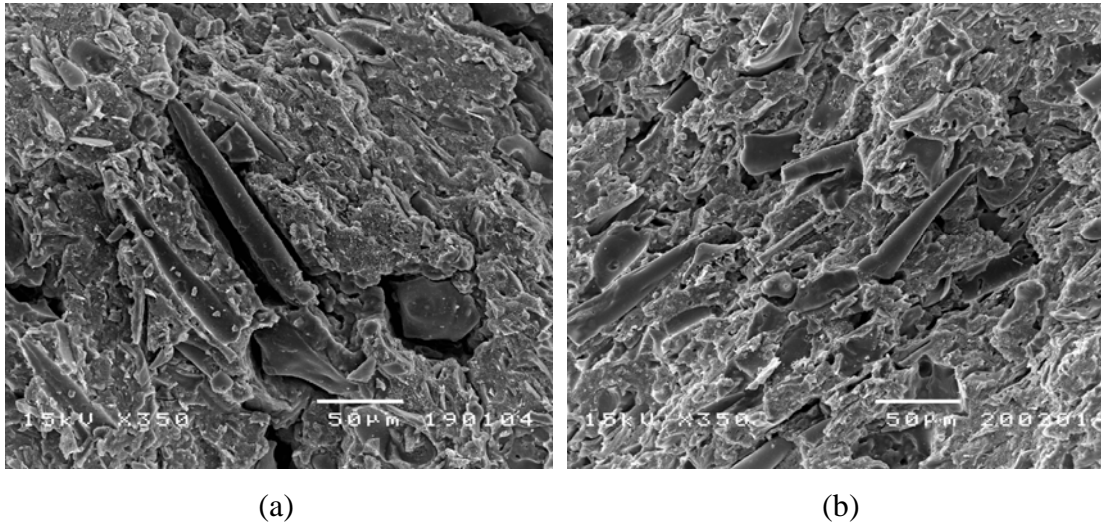


Figure 5.5 The SEM micrographs of the PVC/RHA composites at (a) 20 phr 45 μm and (b) 60 phr 45 μm .

5.1.3 Compressive Properties

The compressive modulus of the PVC compound and the PVC/RHA composites is shown in Figure 5.6. The compressive modulus of the PVC compound was about 1.33 GPa. The compressive modulus of the PVC/RHA composites increased with increasing RHA contents. Compared with the PVC compound, the compressive modulus of the PVC/RHA composites with 20, 40, 60 and 80 phr of RHA content increased by approximately 31%, 59.9%, 69.9% and 81.1% respectively. Due to the incorporation of the rigid RHA particles which predominantly consist of silica, the compressive modulus of the composites increased similar to the tensile and the flexural modulus.

Figure 5.7 illustrates the compressive strength of the PVC/RHA composites. The compressive strength of PVC compound which was about 37.50 MPa had lower than those of all the PVC/RHA composites. The compressive strength of the composites clearly increased with increasing RHA contents by increasing to 46.02 and 60.68 MPa at 20 and 80 phr of RHA contents respectively.

In the case of RHA particles sizes, the compressive modulus and the compressive strength of the PVC/RHA composites with fine RHA particles were not significantly different from those of the composites with large RHA particles.

The compressive strength of the PVC/RHA composites with 20 to 80 phr which was about 43.2 - 60.7 MPa was in range of the compressive strength of natural wood (between 14.1 - 70.2 MPa) [63]. This indicated that the PVC/RHA composites can be used as WPCs to replace natural wood in application under compression load.

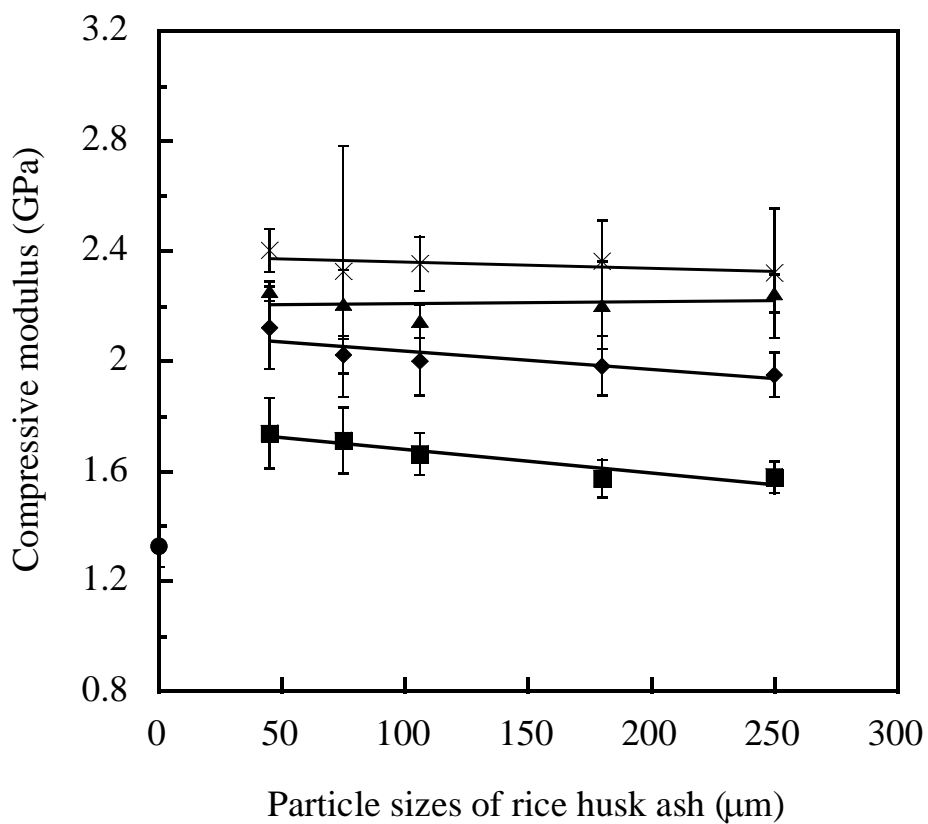


Figure 5.6 RHA contents on the compressive modulus of the PVC/RHA composites with various at 0 phr (●), 20 phr (■), 40 phr (◆), 60 phr (▲) and 80 phr (×) and different RHA particle sizes.

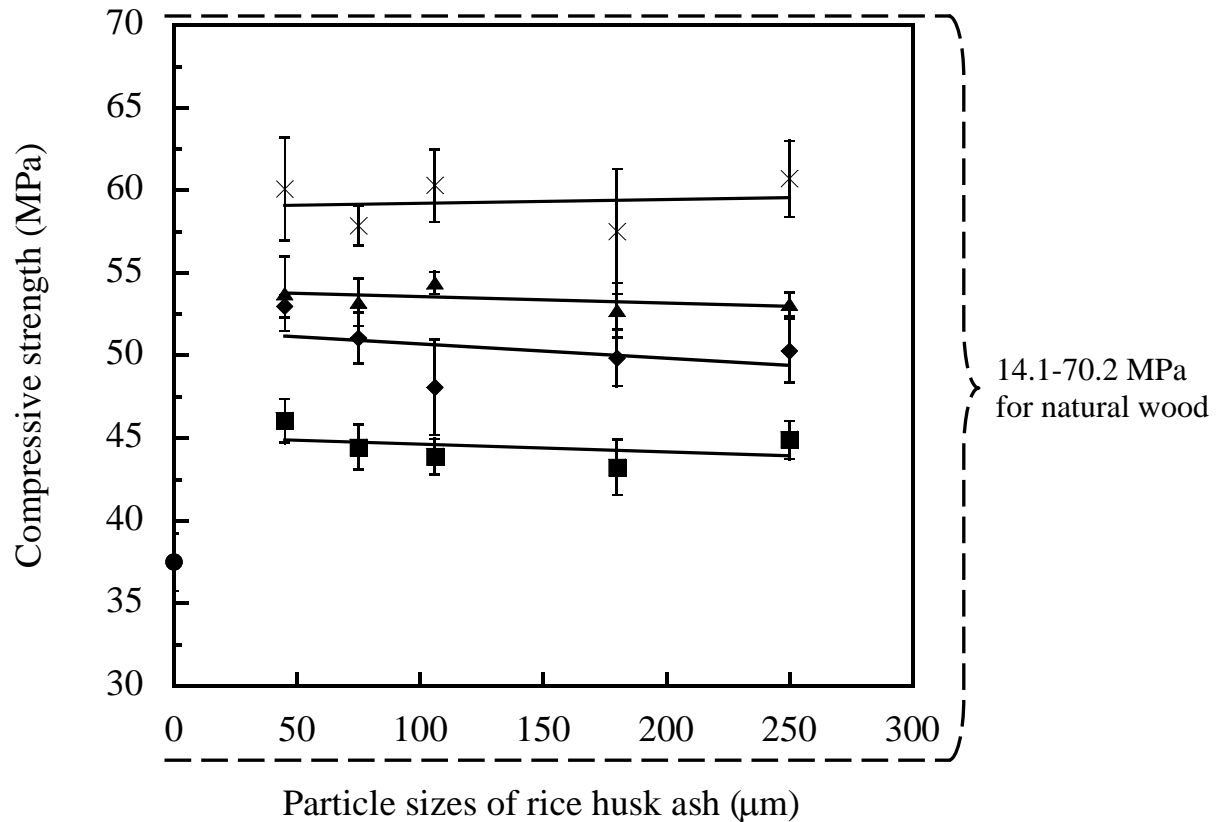


Figure 5.7 RHA contents on the compressive strength of the PVC/RHA composites with various at 0 phr (●), 20 phr (■), 40 phr (◆), 60 phr (▲) and 80 phr (×) and different RHA particle sizes.

5.1.4 Impact Properties

Figure 5.8 demonstrates the notched Izod impact energy and strength of the PVC/RHA composites. The impact energy of the composites decreased with greater RHA contents. The notched Izod impact energy of PVC compound was 12.10 kJ/m², whereas the impact energy of all PVC/RHA composites were reduced from PVC compound at approximately 27.7%, 38.0%, 42.5% and 46.7% in the 20, 40, 60 and 80 phr of RHA respectively. This is in agreement with Fuad et al. [42] who studied the effects of white rice husk ash (WRHA) on the mechanical properties of the polypropylene (PP)/WRHA composites. They found that the impact energy of the PP/WRHA composites decreased with WRHA content by decreasing to 23% at 40 % by weight of WRHA compared with those of the PP/WRHA composites. The

reduction of the impact energy of the PVC/RHA composites can be explained that the RHA filled in the PVC matrix causes the composites to be stiffer. The ductile portion of PVC matrix was reduced, thus decreasing the composite toughness.

In case of RHA particle sizes, the impact energy of the PVC/RHA composites increased slightly with the larger RHA particles. This is because the small RHA particles have the larger surface areas which conduct to create many poor interfacial adhesions or voids between the PVC matrix and the RHA particles as shown in Figure 5.9. The voids led to easier crack propagation along the interface upon impact.

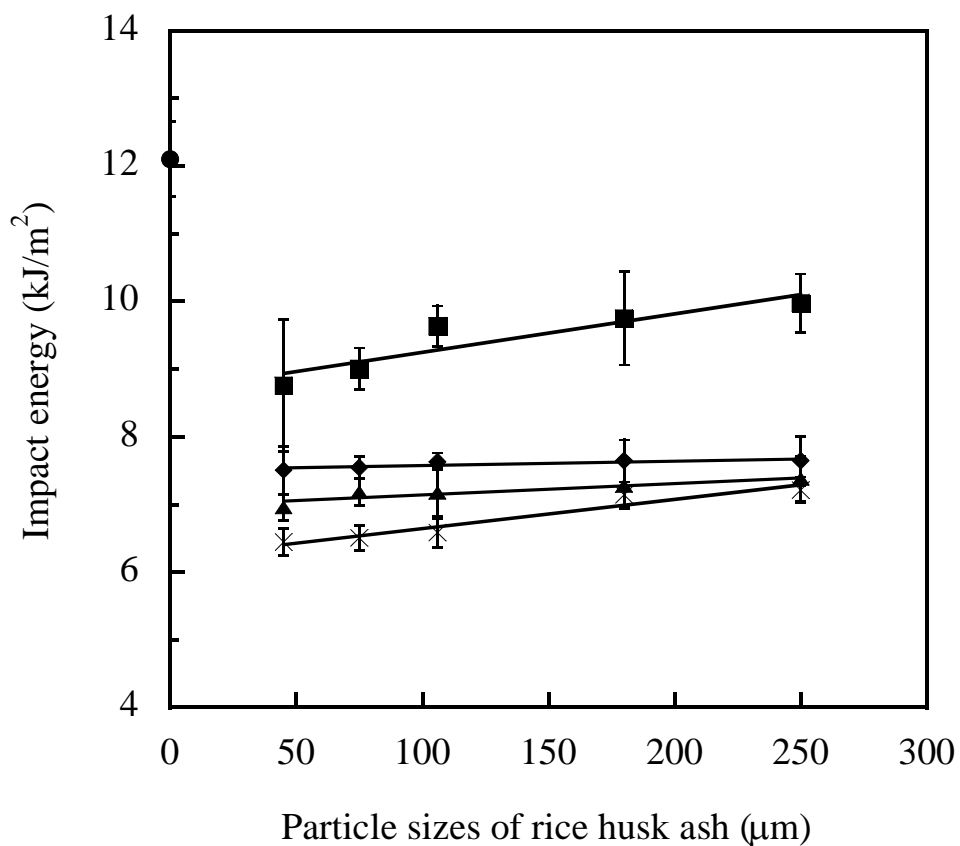
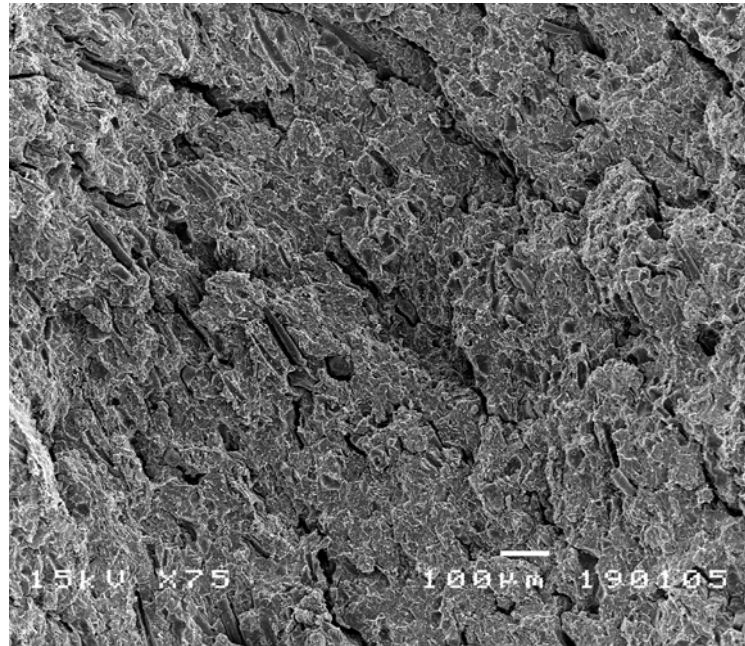
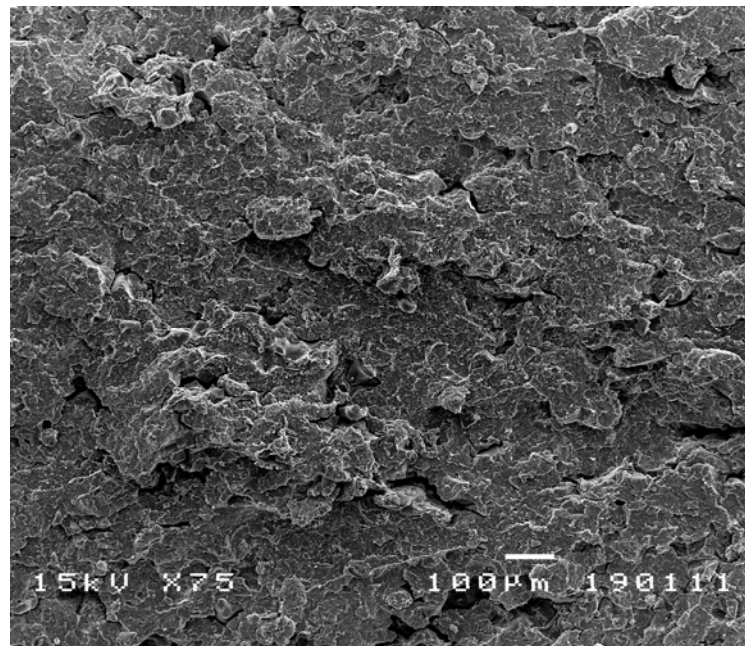


Figure 5.8 RHA contents on the notched Izod impact energy of the PVC/RHA composites with various at 0 phr (●), 20 phr (■), 40 phr (◆), 60 phr (▲) and 80 phr (×) and different RHA particle sizes.



(a)



(b)

Figure 5.9 The SEM micrographs of the PVC/RHA composites at (a) 20 phr 45 μm and (b) 20 phr 180 μm .

5.2 Thermal Properties of the PVC/RHA Composites

5.2.1 Heat Deflection Temperature (HDT)

The results of HDT of the PVC/RHA composites show in Table 5.1. It was found RHA had small effect on the HDT of the PVC/RHA composites. The HDT of the PVC compound was 78 °C. When RHA was added, the HDT of the composites tended to increase slightly with greater RHA contents by increasing to 82 °C at 80 phr. This is because the mobility of the PVC molecules was restricted by the rigid RHA particles. Therefore, the PVC/RHA composites with greater RHA content can more resist heat deflection. However, the particle sizes of RHA had no significant effect on the HDT of the PVC/RHA composites.

Table 5.1 Heat deflection temperature of the PVC/RHA composites.

Particle sizes (μm)	Heat deflection temperature ($^{\circ}\text{C}$)			
	20 phr	40 phr	60 phr	80 phr
45	79	80	81	82
250	79	81	81	82

* Heat deflection temperature of PVC compound is 78 °C.

5.2.2 Glass Transition Temperature (T_g)

Generally, glass transition temperature (T_g) is one of the thermal properties which are able to exhibit the temperature range for application of materials. The higher glass transition temperature means that the material can be used in higher temperature without being rubber-like. For example, Acrylonitrile butadiene styrene (ABS, $T_g = 110\text{ }^{\circ}\text{C}$) is rigid and can be used for high-strength application when the temperature is as high as 100°C . Comparatively, at a such temperature, high density polyethylene (HDPE, $T_g = -125\text{ }^{\circ}\text{C}$) cannot provide high strength and becomes

rubber-like. In this research, the T_g 's are obtained from the loss tangent ($\tan \delta$) of dynamic mechanical analysis (DMA).

Table 5.2 compares the T_g 's of the PVC/RHA composites at various RHA contents (from 20 phr to 80 phr) and particle sizes (45 μm and 250 μm). It can be observed that the T_g 's of the composites are higher than that of the PVC compound (91 °C) for both particle sizes. There is no significant difference between the T_g 's of the PVC/RHA composites with different particle size. Interestingly, the T_g 's of the composites tend to be increased with increasing RHA contents. The T_g of the composites with RHA at 20 and 80 phr increased by about 4 and 7 °C, respectively in comparison with that of the PVC compound.

The possible reason to explain this phenomenon is that RHA, mainly consisting of silicon dioxide, is stiff. It possibly has an effect on hindering the mobility of the PVC molecules, leading to an increase in the T_g of the composites. This phenomenon is in agreement with Wan et al. [65]. They studied the thermal properties of PVC/montmorillonite nanocomposite. It was reported that the filler is able to increase the T_g of PVC from 85.3 °C to 87.6 °C. As the same reason as this study, the filler prevents the segmental motion of the polymer chains. However, the particle sizes of RHA had no significant influences on the T_g of the composites.

Table 5.2 Glass transition temperature of PVC/RHA composites.

Particle size (μm)	Glass transition temperature (°C)			
	20 phr	40 phr	60 phr	80 phr
45	95	95	97	98
250	94	95	96	97

*Glass transition temperature of PVC compound is 91 °C.

5.2.3 Thermogravimetric Analysis

The TGA thermograms of RHA, the PVC compound, and the PVC/RHA composites are shown in Figure 5.10. The TGA thermograms indicated that RHA was thermally stable and did not degrade at all over the temperature range studied whereas the TGA curve of the PVC compound exhibited two ranges of decomposition. The first range at 260-360 °C associated with the decomposition of PVC releasing HCl [66], about 55 % of weight loss, while the second range at 360-510 °C corresponded to the decomposition of the several additives and organics within the PVC, leaving a residue char weight of 17 %. Similarly, the PVC/RHA composites were decomposed at two temperature ranges, 260-360 °C and 360-510 °C, as same as the PVC compound. At first decomposition range, the weight loss of the composites was 48 and 34 % at 20 and 80 phr respectively. The weight loss of the composites decreased with greater RHA content because the PVC compound which was decomposed in this range had lower content. Moreover, the residue weight of the PVC/RHA composites increased with increasing RHA contents. The residue weights of the PVC/RHA composites at 20 and 80 phr were 25 and 47 wt% respectively. The particle sizes of RHA had no significant effects on the T_d and the residue weights of the PVC/RHA composites.

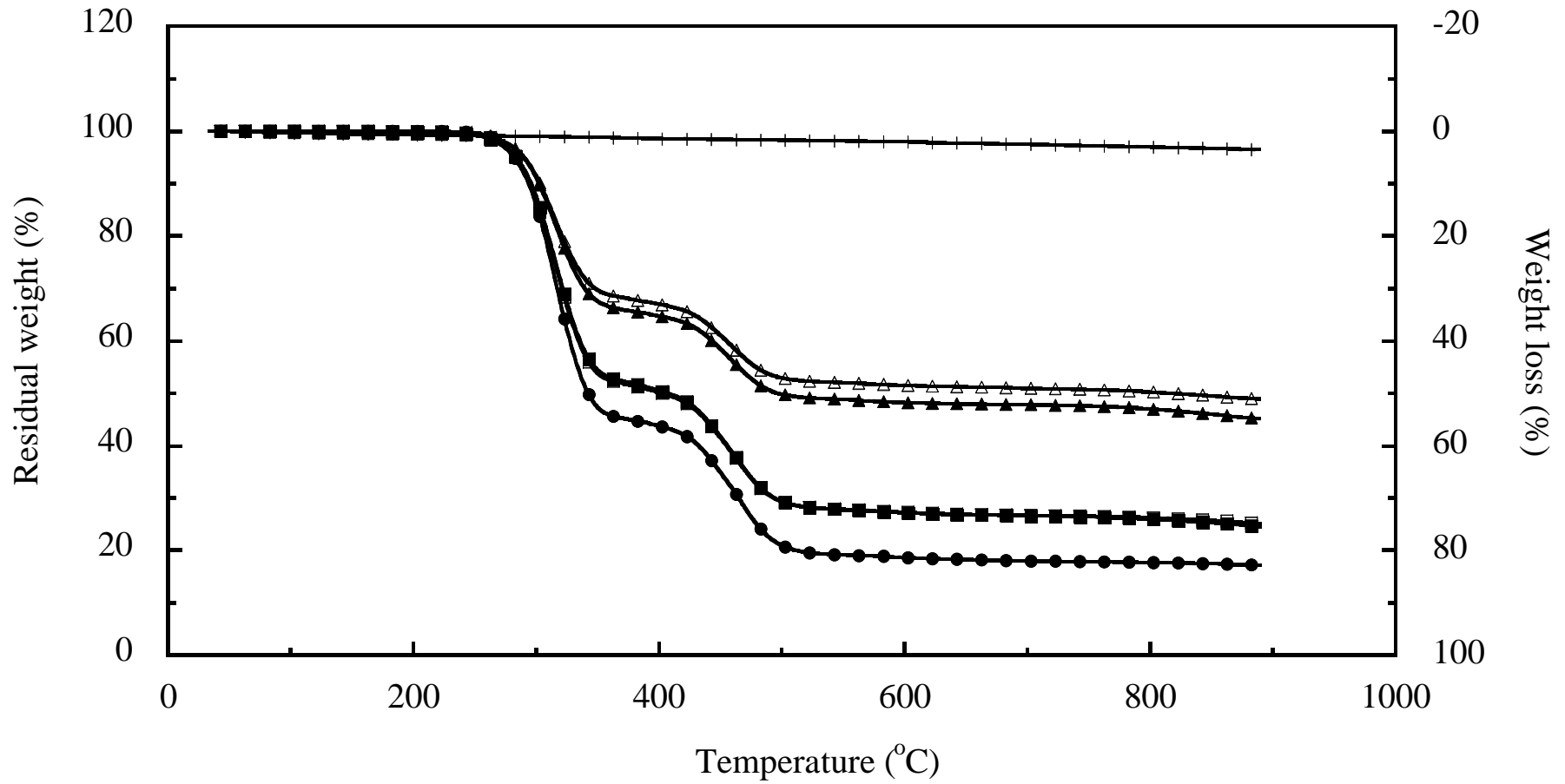


Figure 5.10 TGA thermograms of the PVC compound (●), RHA (+) and the PVC/RHA composites: 20 phr 45 μm (■), 20 phr 250 μm (□), 80 phr 45 μm (▲) and 80 phr 250 μm (△).

5.3 Physical Properties of the PVC/RHA Composites

5.3.1 Density

Figure 5.11 illustrates the density of the PVC compound and the PVC/RHA composites. Density of the PVC compound and RHA was 1.425 and 1.93 g/cm³ respectively. Density of the PVC/RHA composites tended to increase with greater RHA contents by increasing to approximately 3, 6, 9 and 11 % at 20, 40, 60 and 80 phr of RHA contents respectively. This is due to the incorporation of RHA particles which are more density than the PVC compound.

In the case of RHA particle sizes, density of the PVC/RHA composites with fine RHA particles was not significantly different from those of the composites with large RHA particles.

The density of the PVC/RHA composites with 20 to 80 phr which was about 1.456 - 1.586 g/cm³ was higher than those of commercial PVC/wood composites (between 1.17 - 1.38 g/cm³) [60-62,64] and natural wood (between 0.31 - 0.88 g/cm³) [63].

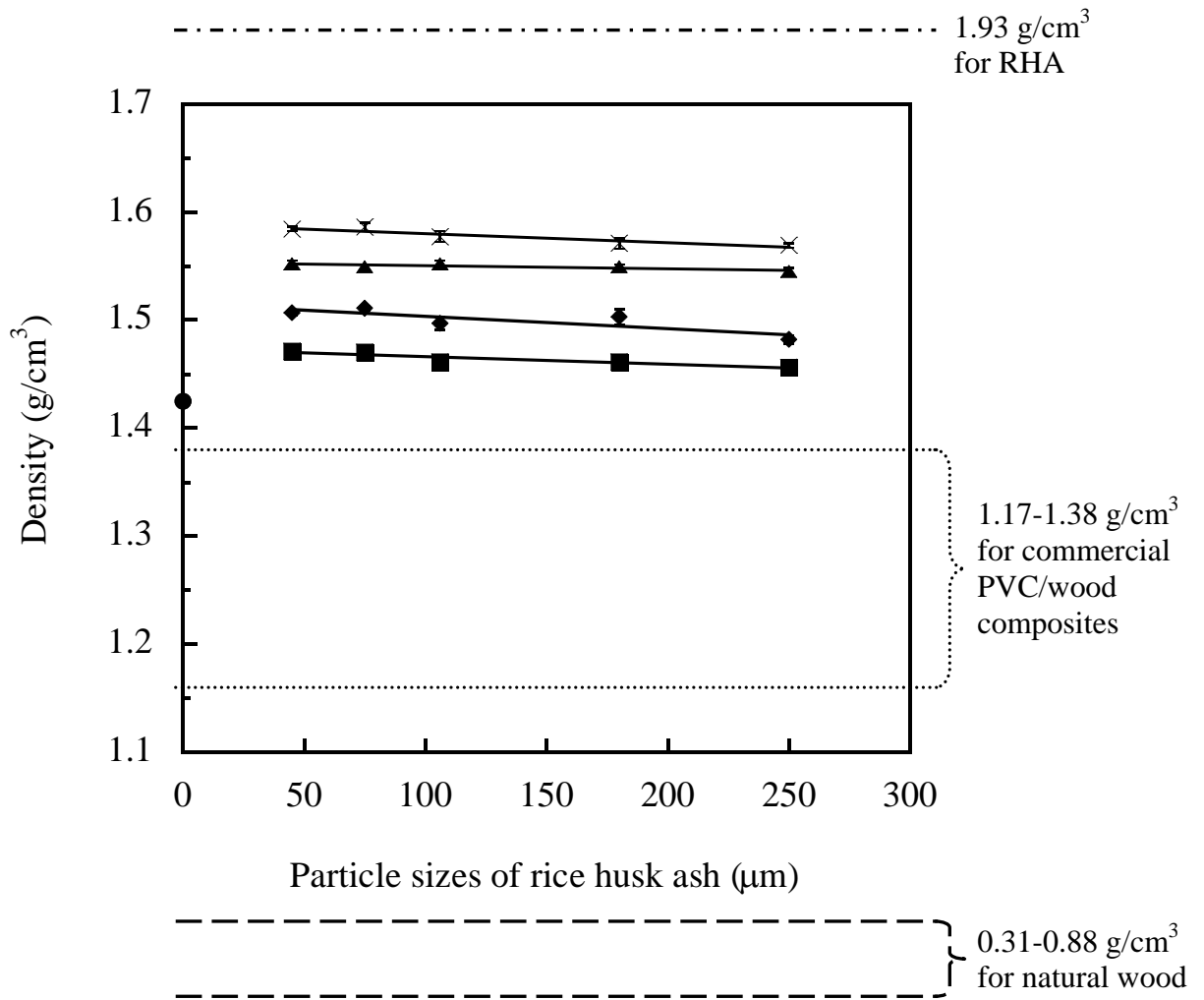


Figure 5.11 RHA contents on density of the PVC/RHA composites with various at 0 phr (●), 20 phr (■), 40 phr (◆), 60 phr (▲) and 80 phr (×) and different RHA particle sizes.

5.3.2 Water Absorption

The RHA had small effect on water absorption of the PVC/RHA composites for 60 days as shown in Figure 5.12-5.14. Figure 5.12 and 5.13 show the water absorption behavior of the PVC compound and the PVC/RHA composites. They indicated that the rate of water absorption of the PVC compound was high at first from the beginning, about seven days, and then the rate of water absorption decreased gradually to saturated stage where the PVC compound cannot absorb more water. Similar to the PVC compound, the PVC/RHA composites had the high rate of

water absorption at the start, about seven days, and then the rate of water absorption of the PVC/RHA composites reduced gradually. Water absorption of the PVC compound sample which was about 0.16% was lower than that of the PVC/RHA composites. From Figure 5.14, the water absorption of the PVC/RHA composites increased with RHA contents by increasing to 0.53%, 0.77%, 1.04%, and 1.35% at 20, 40, 60, and 80 phr respectively. This result may be due to high porosity of the RHA particles, as shown in Figure 5.15. Moreover, poor interfacial adhesion between the PVC matrix and the RHA particles, as shown in Figure 5.5, cause the voids in the composites. These pores and voids can be the positions in the infiltration of water or moisture. As a result, the PVC/RHA composites can absorb more water.

In the case of RHA particle sizes, water absorption of the PVC/RHA composites with small RHA particles was not significantly different from those of the composites with large RHA particles.

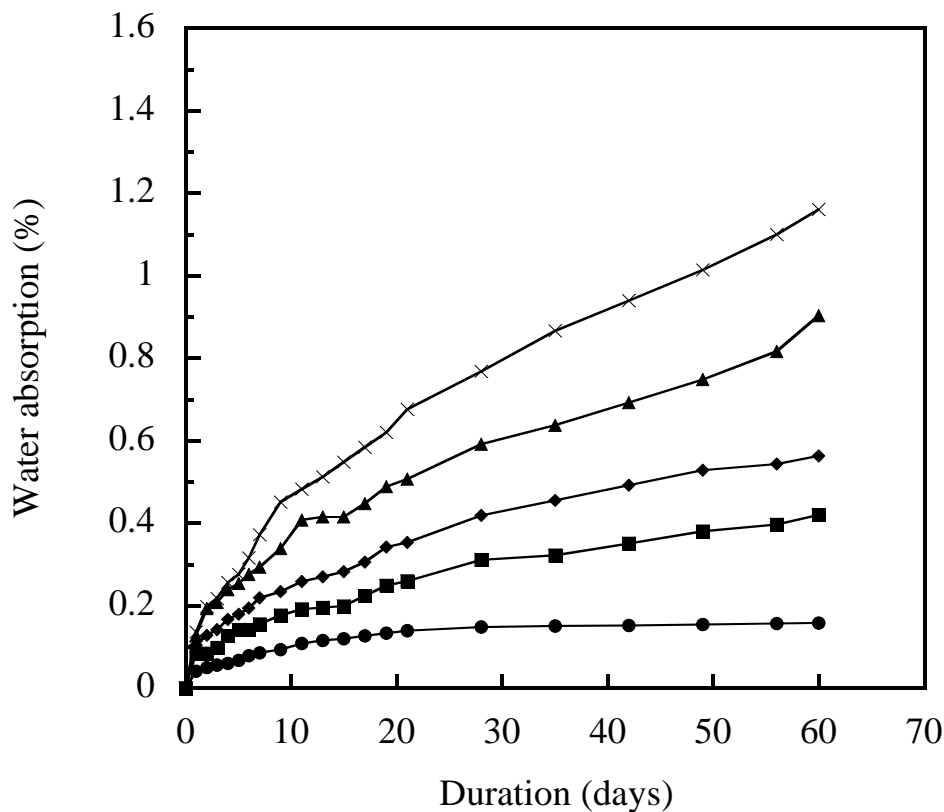


Figure 5.12 Water absorption behavior of the PVC/RHA composites with particle size of 75 μm at 0 phr (●), 20 phr (■), 40 phr (◆), 60 phr (▲) and 80 phr (×).

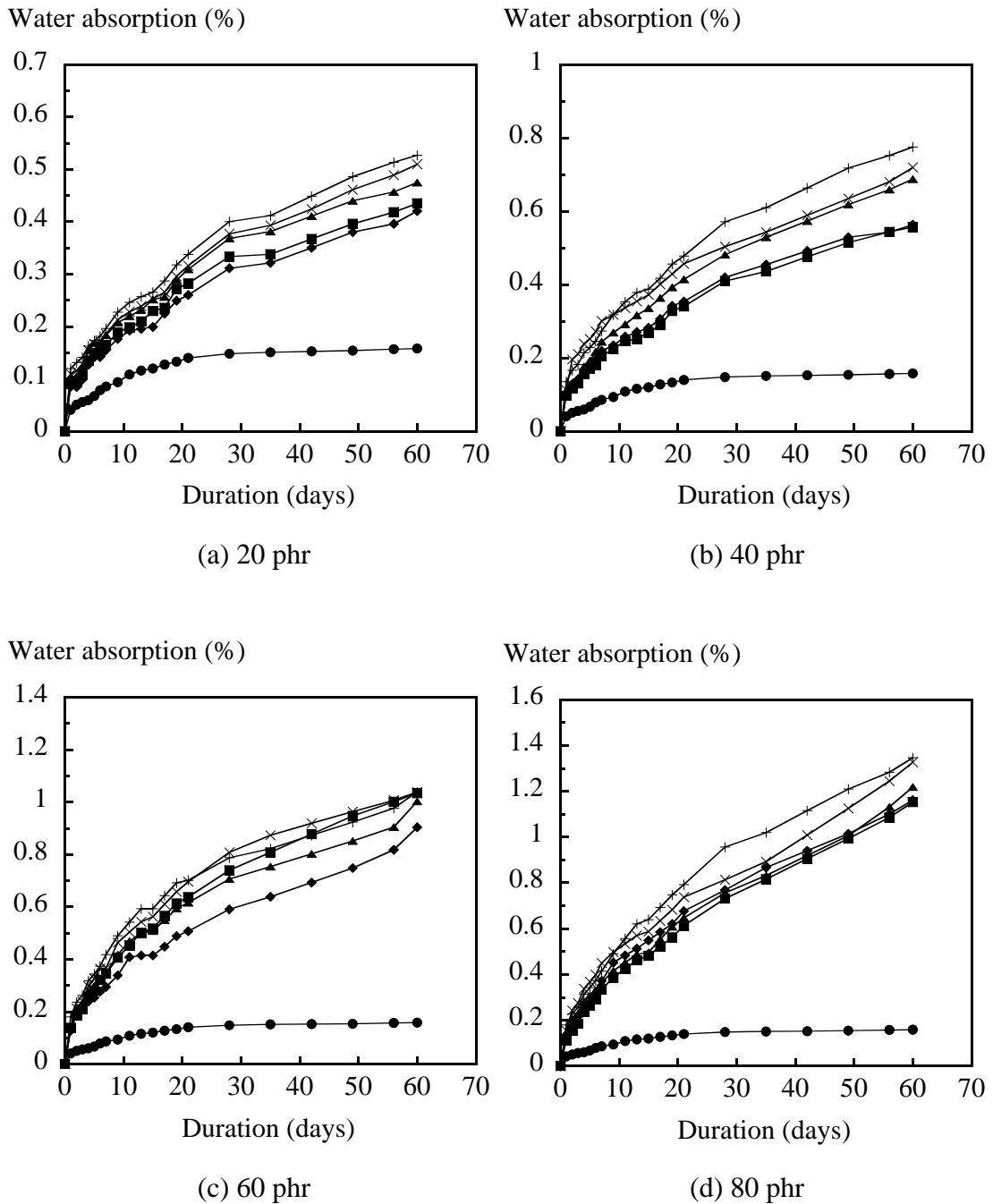


Figure 5.13 Water absorption behavior of the PVC compound (●) and the PVC/RHA composites with RHA particle sizes of 45 μm (■), 75 μm (◆), 106 μm (▲), 180 μm (×) and 250 μm (+) at (a) 20 phr, (b) 40 phr, (c) 60 phr and (d) 80 phr.

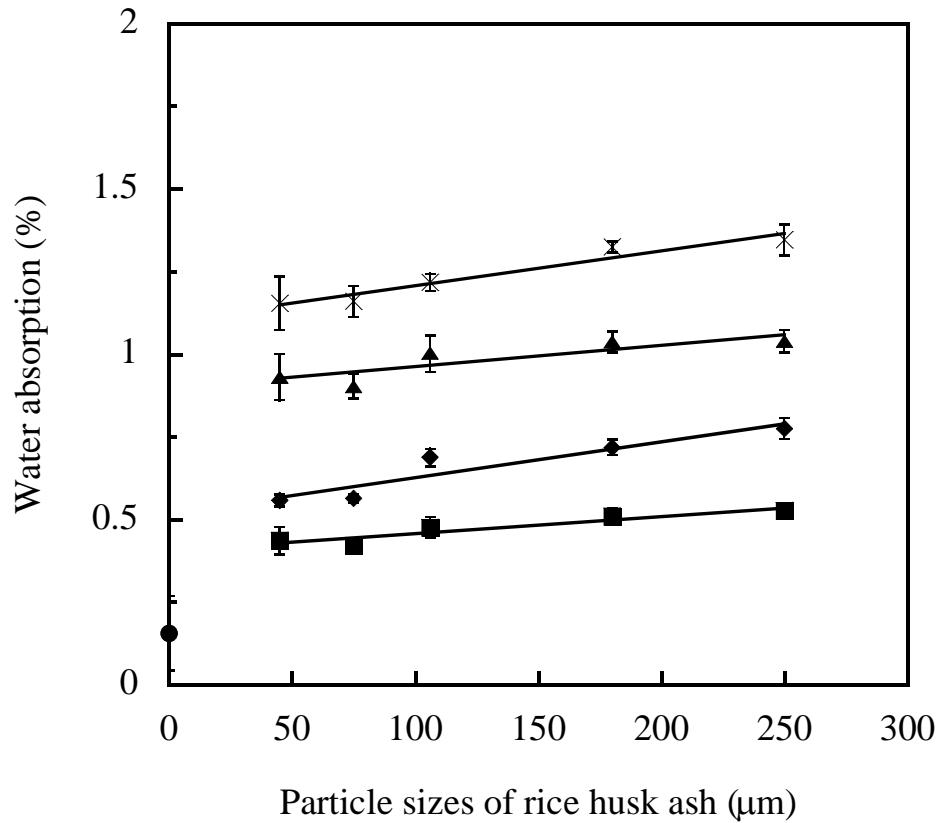


Figure 5.14 Water absorption of the PVC/RHA composites with various at 0 phr (●), 20 phr (■), 40 phr (◆), 60 phr (▲) and 80 phr (×) for different RHA particle sizes after immersion in water for 60 days.

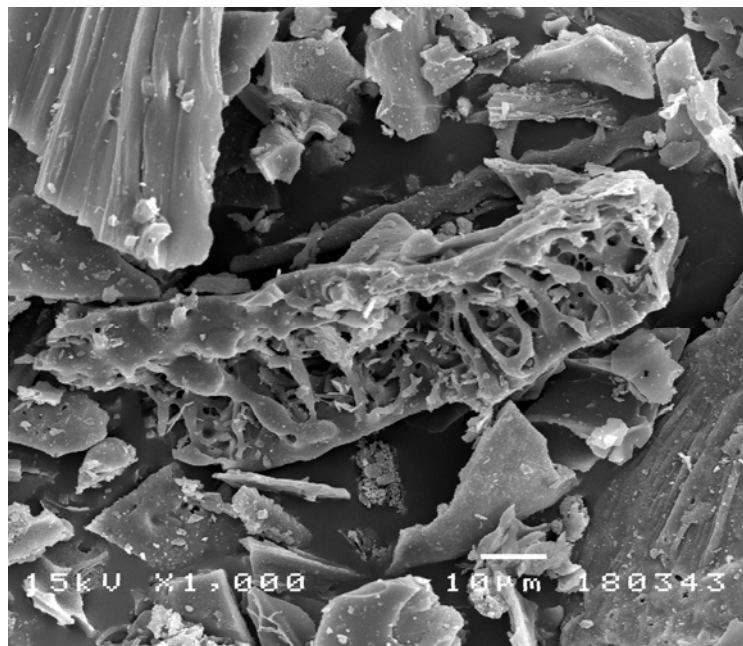
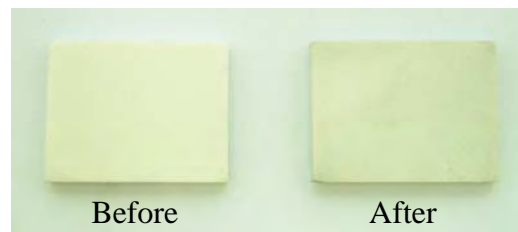


Figure 5.15 Porosity of the RHA particles.

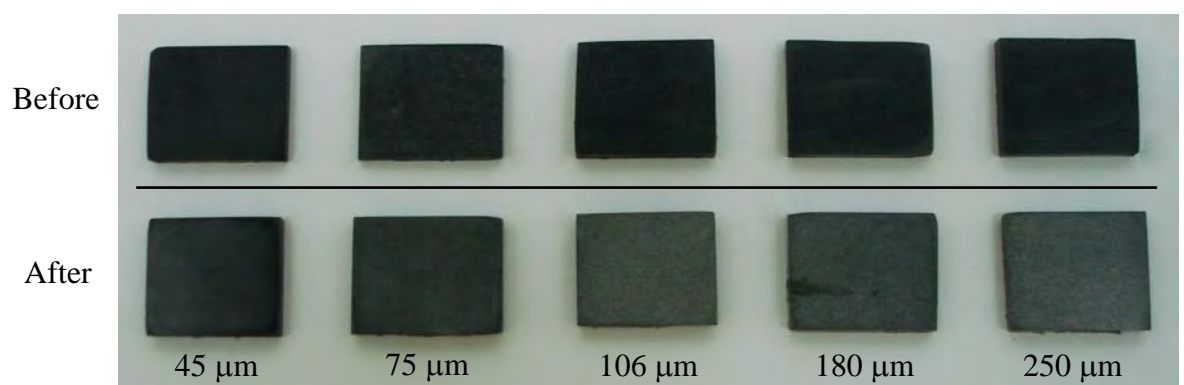
5.3.3 Outdoor Weathering Test

Figure 5.16 compares the appearance of the PVC/RHA composites for different RHA contents and particle sizes before and after outdoor weathering test for 60 days. Before testing, PVC compound sample was found to have white color. In the case of the PVC/RHA composites, the composites show dark grey color at 20 phr. Further increase in the RHA content led to change of color from dark grey to black color. The small RHA particles yield composites with a darker shade than those with larger RHA particles.

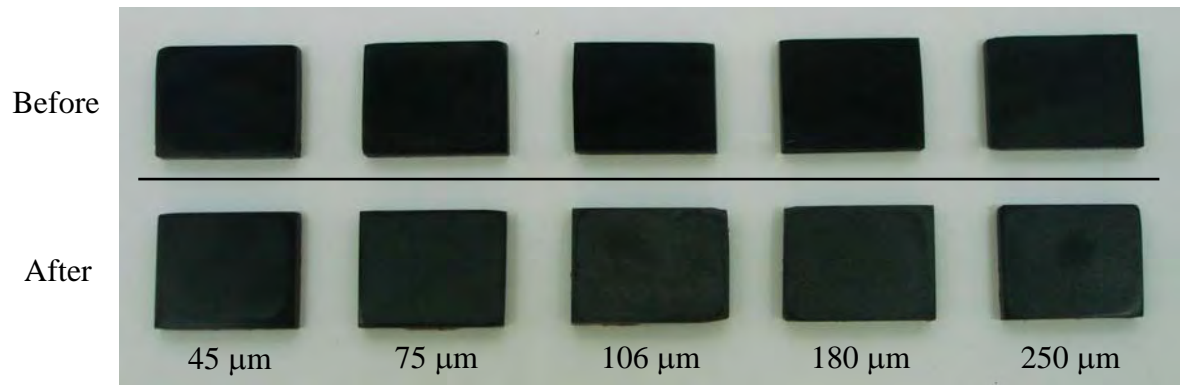
After outdoor weather exposure for 30 days, PVC compound showed light yellow color. Moreover, the color of the PVC/RHA composites was found to clearly pale at 20 and 40 phr of RHA content. However, the color of the composites with 60 and 80 phr were found to slightly pale.



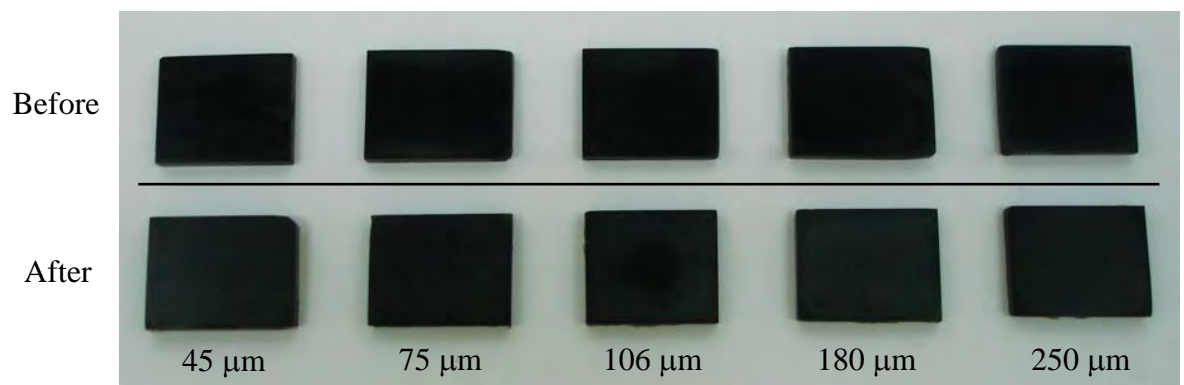
(a) PVC compound



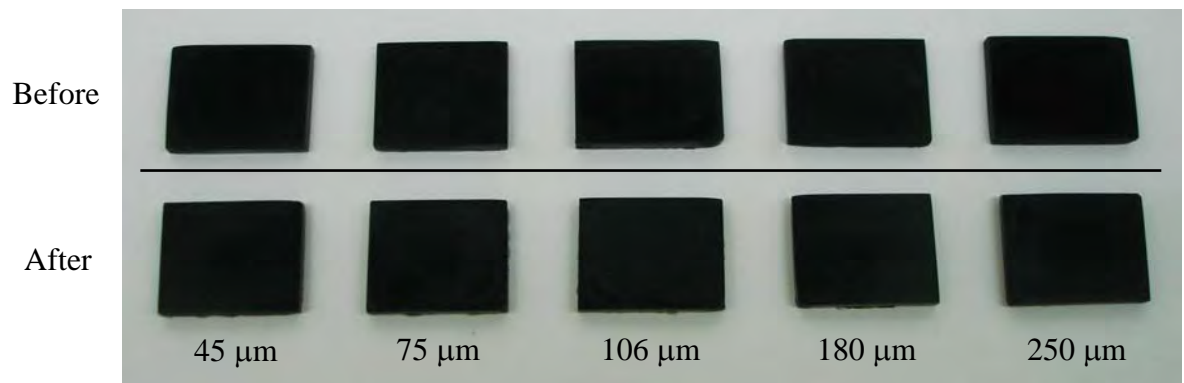
(b) 20 phr



(c) 40 phr



(d) 60 phr



(e) 80 phr

Figure 5.16 The appearance of the PVC/RHA composites before and after outdoor weathering test for 60 days: (a) 0 phr, (b) 20 phr, (c) 40 phr, (d) 60 phr and (e) 80 phr.

5.4 Morphological Characterization of the PVC/RHA Composites

In this study, the PVC/RHA composites were cracked at cryogenics for fracture surfaces observation. The morphology of the PVC/RHA composites at different RHA contents and particle sizes are shown in Figure 5.17. The SEM micrographs of the composites exhibit that the poor interfacial adhesions between the PVC matrix and the RHA particles possibly cause the voids in the PVC/RHA composites, resulting in the reduction of the tensile and flexural strength of the composites. Figure 5.17(a) and 5.17(b) show the interface between the matrix and the filler in the PVC/RHA composites at 20 phr. Moreover, the composites with greater RHA content, as shown in Figure 5.17(c) and 5.17(d), had more agglomeration of the RHA particles in the PVC matrix. However, the composites with larger RHA particles had better disperse in the PVC matrix than that with smaller RHA particles as shown in Figure 5.18(a) and 5.18(b).

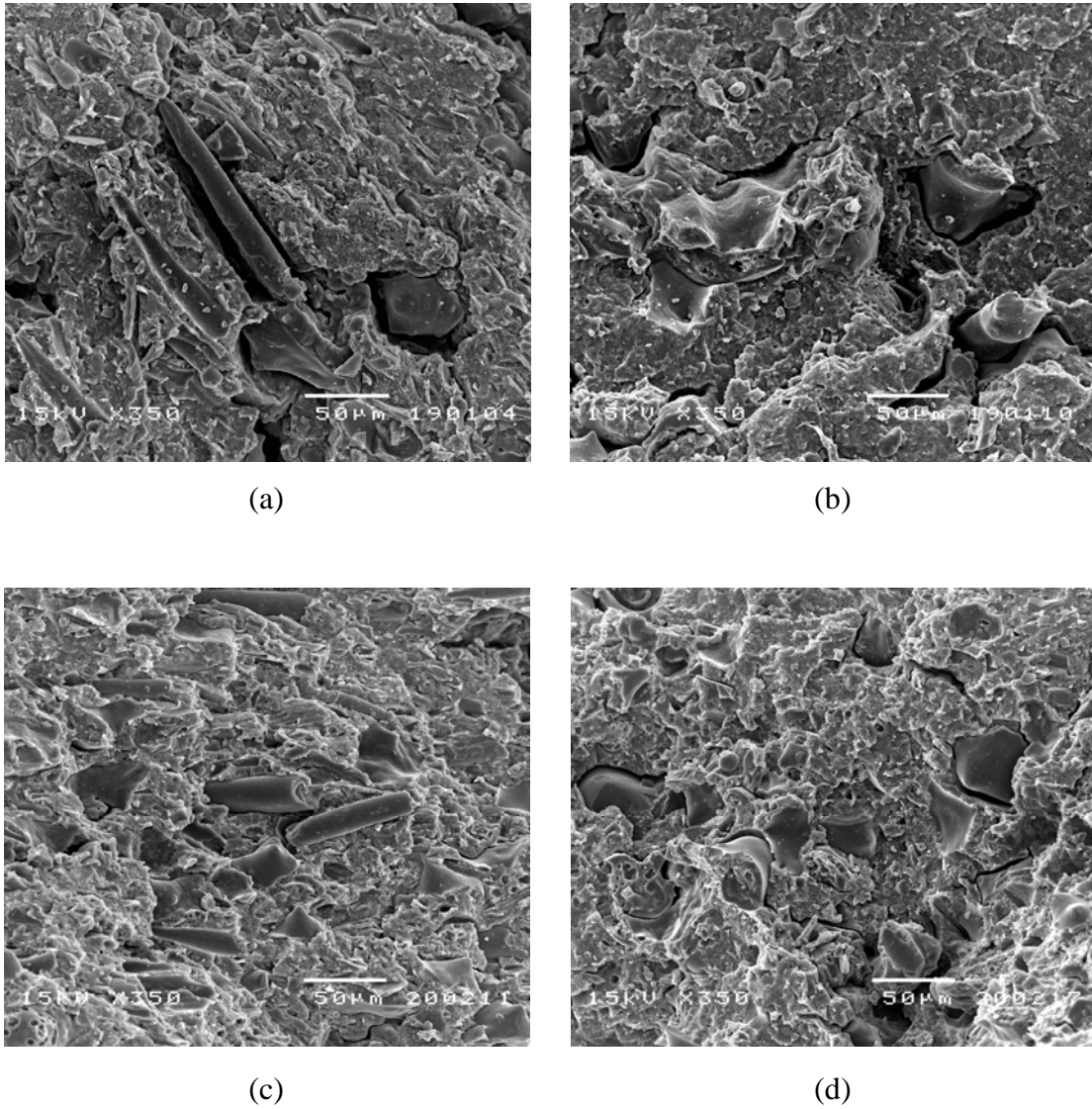


Figure 5.17 The SEM micrographs of the PVC/RHA composites at high magnification of: (a) 20 phr 45 μm , (b) 20 phr 180 μm , (c) 80 phr 45 μm and (d) 80 phr 180 μm .

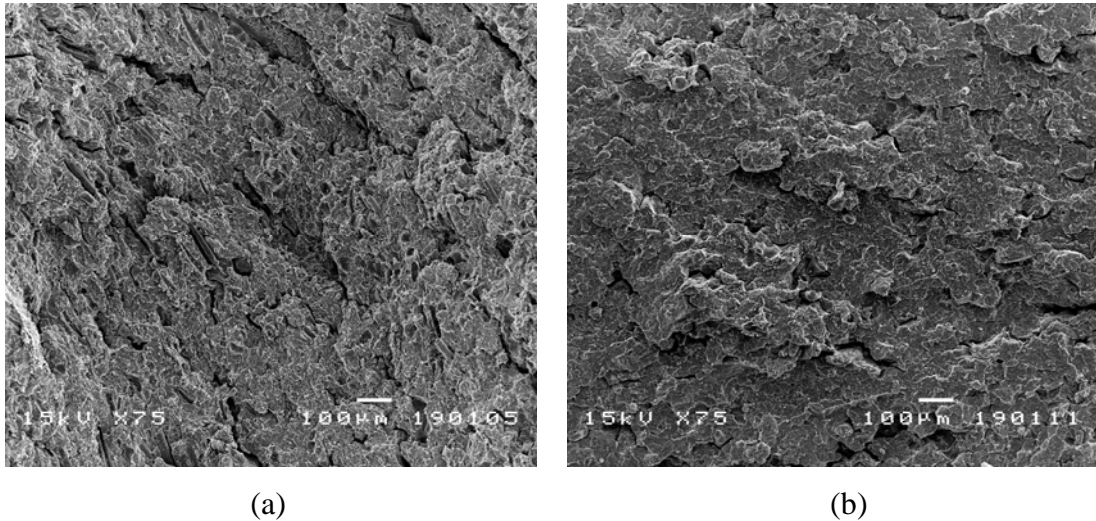


Figure 5.18 The SEM micrographs of the PVC/RHA composites at low magnification of: (a) 20 phr 45 μm and (b) 20 phr 180 μm .

5.5 Cost Analysis of the PVC/RHA Composites

The cost analysis of the PVC/RHA composites is shown in Table 5.3. The cost of the PVC/RHA composites decreased with increasing RHA contents. The raw material costs of the PVC compound (K66) and the RHA were 41.32 and 4 Bahts/kg respectively. The raw material cost of the composites with 20 phr of RHA contents was 36.15 Baht/kg. When RHA was added at 40, 60 and 80 phr, the cost of the PVC/RHA composites reduced by approximately 10.82%, 19.29% and 26.11% respectively. Moreover, the raw material cost of commercial PVC/wood composites was 41 Bahts/kg which was more expensive than those of the PVC/RHA composites. This result indicated that the use of RHA as a filler in WPCs can reduce the raw material cost of WPCs. As a result, the price of WPCs is decreased.

Table 5.3 Cost analysis of the PVC/RHA composites [67-68].

Materials	Price (Baht/kg)	Weight (kg)			
		20 phr	40 phr	60 phr	80 phr
PVC compound (K66)	41.32	0.8615	0.7567	0.6746	0.6086
Rice husk ash	4.00	0.1385	0.2433	0.3254	0.3914
Cost (Baht/Kg)		<u>36.15</u>	<u>32.24</u>	<u>29.18</u>	<u>26.71</u>

* Raw material cost of commercial PVC/wood composites was 41 Bahts/kg [67].

CHAPTER VI

CONCLUSIONS AND RECOMMENDATIONS FOR FURTHER STUDIES

6.1 Conclusions

The effects of rice husk ash (RHA) contents and its particle sizes on the mechanical, thermal and physical properties of the PVC/RHA composites were investigated. The current research can be concluded as follow:

i) With increasing in RHA contents, the tensile, flexural and compressive modulus and compressive strength of the PVC/RHA composites increased because RHA made composites stiffer.

ii) Both tensile and flexural strengths of the composites tended to decrease with increasing RHA contents. This is due to poor interfacial bonding between the PVC matrix and the RHA particles.

iii) As greater RHA contents, the impact energy decreased because the toughness of the PVC/RHA composites was decreased.

iv) The HDT and the T_g 's of the PVC/RHA composites increased slightly with increasing RHA contents. This is because the mobility of the PVC molecules was hindered by RHA particles.

v) RHA had no significant effect on the T_d of the composites while the residue weight increased with greater RHA contents.

vi) Density and water absorption of the PVC/RHA composites increased with higher RHA contents.

vii) The PVC/RHA composites show dark grey color at 20 phr. Further increase in the RHA content led to change of color from dark grey to black color. Moreover, the small RHA particles yield composites with a darker shade than those with larger RHA particles. After outdoor weather exposure for 30 days, the color of the composites was paled.

viii) The SEM micrographs showed the poor interfacial adhesions between the phases of the PVC matrix and the RHA fillers.

ix) The particle sizes of RHA had no significant effect on the tensile, flexural and compressive properties (modulus and strength) while the impact energy increased with larger RHA particles.

x) The HDT, T_g , T_d , density and water absorption of the PVC/RHA composites with fine RHA particles were not significantly different from those of the composites with large RHA particles.

xi) The PVC/RHA composites can be used to substitute natural wood in application of WPCs under tension and compression load.

6.2 Recommendations for Further Studies

i) Improvement of the interfacial adhesion between the PVC matrix and the RHA by application of a coupling agent is recommended as an extension of the present study. It is anticipated that the mechanical properties would be improved.

ii) Investigation of the effect of environment such as water absorption or weather on the mechanical properties is recommended as a further study.

iii) Incorporation of blowing agents to produce the PVC/RHA foamed composites is also recommended as a way to reduce the weight of the WPC.

iv) Others commodity plastics such as PE or PP may be used to replace the PVC matrix.

REFERENCES

- [1] Cunningham, J. Annual Review and Assessment of the World Timber Situation 2006. International Tropical Timber Organization (ITTO), 2006.
- [2] Mali, J.; Sarsama, P.; Suomi-Lindberg, L.; Metsa-Kortelainen, S.; Peltonen, J.; Vilkki, M.; Koto, T.; and Tiisala, S. Woodfibre-plastic composites. VTT Technical Research Centre of Finland, 2003.
- [3] Smith, R. The environmental aspects of the use of PVC in building products. 2nd edition. CSIRO Molecular Science, 1998.
- [4] Vinylthai: All About PVC [Online], Available:
<http://www.vinylthai.co.th/static/wma/pdf/8/8/3/1/All%20About%20PVC.pdf> [19 February 2008].
- [5] Powell, P. C. Engineering with fibre-polymer laminates. London : Chapman & Hall, 1994.
- [6] Mishra, S.; Mohanty, A. K.; Drzal, L. T.; Misra, M. and Parija, S. Studies on mechanical performance of biofibre/glass reinforced polyester hybrid composites. Composites Science and Technology 63 (2003) : 1377-1385.
- [7] Reinhart, T. J. and Clements, L. L. Engineering materials handbook. Ohio : ASM International, 1989.
- [8] Hilling, W. B. Composite Materials. Encyclopedia of Chemical Technology 6 (1981) : 683-699.
- [9] Gachter, R. and Muller H. Plastic additive handbook. New York : Houser Pulishers, 1987.
- [10] Sperling, L. H. Introduction to physical polymer science. New York : John Wiley & Sons, 1992.
- [11] Weeton, J. W.; Peters, D. M. and Thomas, K. L. Engineers' Guide to Composite Materials. Ohio : American Society for Metals, 1987.
- [12] Hull, D. An Introduction to Composite Materials. Cambridge : Great Britain at the University Press, 1990.
- [13] Matthews, F. L. and Rawlings, R. D. Composite Materials: Engineering and Science. 1st edition. London : Chapman & Hill, 1994.

- [14] Titow, W. V. PVC Technology. 4th edition. New York : Elsevier Applied Science Publishers, 1984.
- [15] Nass, L. I. and Heiberger, C. A. Encyclopedia of PVC. Vol. I: Resin Manufacture and Properties. 2nd edition. Revise and expanded. New York : Marcel Dekker, 1985.
- [16] Klyosov, A. A. Wood-Plastic Composites. New Jersey : John Wiley & Sons, 2007.
- [17] Vinythai: Variety of PVC Products: PVC & Additives [Online], Available: <http://www.vinythai.co.th/static/wma/pdf/8/8/3/3/variety%20pvc%20and%20additives.pdf> [19 February 2008].
- [18] Birley, A. W.; Heath, R. J. Plastics Materials: Properties and Applications. 2nd edition. New York : Chapman and Hall, 1988.
- [19] Gomez, I. L. Engineering with Rigid PVC: Processability and Applications. New York : Marcel Dekker, 1984.
- [20] Krishnarao, R. V.; Subrahmanyam, J. and Kumar, T. J. Studies on the formation of black particles in rice husk silica ash. Journal of the European Ceramic Society 21 (2001) : 99-104.
- [21] Ismail, H.; Nizam, J. M. and Abdul Khalil, H. P. S. The effect of a compatibilizer on the mechanical properties and mass swell of white rice husk ash filled natural rubber/linear low density polyethylene blends. Polymer Testing 20 (2001) : 125-133.
- [22] Bronzeoak Ltd. Rice husk ash market study. Limited Distribution – UK Companies only, 2003.
- [23] Houston, D. F. Rice Hulls. Rice Chemistry and Technology. American Association of Cereal Chemist, 1972.
- [24] Clemons, C. Wood-Plastic Composites in the United States: The Interfacing of Two Industries. Journal Forest Products 52 (2002) : 10-18.
- [25] Morton-Jones, D. H. Polymer processing. New York : Chapman and Hall, 1987.
- [26] Two-roll mill [Online], Available: <http://www.sut.ac.th/Engineering/Polymer/tworollmill.htm> [5 March 2008].
- [27] Mansion, J. A., and Sperling, L. H. Polymer blend and composites. New York : Plenum Press, 1976.

- [28] Compression molding [Online], Available:
http://www.substech.com/dokuwiki/doku.php?id=closed_mold_fabrication_of_polymer_matrix_composites [5 March 2008].
- [29] Hernandez, R. J.; Selke, S. E. M. and Culter, J. D. Plastics Packaging. Hanser Gardner Publications, 2000.
- [30] Tensile Testing [Online], Available:
http://www.instron.co.th/wa/applications/test_types/tension/default.aspx
[19 March 2008].
- [31] Flexural Testng [Online], Available:
http://www.instron.us/wa/applications/test_types/flexure/default.aspx
[19 March 2008].
- [32] Flexural Properties [Online], Available:
<http://www.ptli.com/testlopedia/tests/Flex-D790.asp> [19 March 2008].
- [33] ASTM D 790 – 03 Standard Test Methods for Flexural Properties of Unreinforced and Reinforced Plastics and Electrical Insulating Materials, 2003.
- [34] Compression Test [Online], Available:
http://www.instron.us/wa/applications/test_types/compression.aspx
[19 March 2008].
- [35] Compressive Strength Testing of Plastics [Online], Available:
<http://www.matweb.com/reference/compressivestrength.aspx>
[19 March 2008].
- [36] Izod Test [Online], Available:
<http://www.azom.com/details.asp?ArticleID=2765> [19 March 2008].
- [37] Izod Impact Strength Testing of Plastics [Online], Available:
<http://www.matweb.com/reference/izod-impact.aspx> [19 March 2008].
- [38] ASTM D 256 – 06 Standard Test Methods for Determining the Izod Pendulum Impact Resistance of Plastics, 2006.
- [39] Fried, J. R. Polymer science and technology. 2nd edition. New Jersey : Prentice Hall, 2003.
- [40] Dynamic mechanical analysis [Online], Available:
http://en.wikipedia.org/wiki/Dynamic_mechanical_analysis
[19 March 2008].

- [41] Cheremisinoff, N. P. Product Design and Testing of Polymeric Materials. New York and Basel : Marcel Dekker, 1990
- [42] Fuad, M. Y. A.; Ismail, Z.; Ishak, Z. A. M.; and Omar, A. K. M. Application of rice husk ash as fillers in polypropylene: Effect of titanate, zirconate and silane coupling agents. Eur. Polym. J. 31 (1995) : 885-893.
- [43] Ismail, H.; Nasaruddin, M. N. and Ishiaku, U. S. White rice husk ash filled natural rubber compounds: the effect of multifunction additive and silane coupling agents. Polymer Testing 18 (1999) : 287-298.
- [44] Hassan, A. B.; Kannan, S. K.; Mohd, M. F. B.; and Zakaria, A. B. Acrylic and CPE modified PVC-U composites - Effect of rice husk ash on impact properties. 15th Symposium of Malaysian Chemical Engineers (2001) : 242-250.
- [45] Yang, H. S.; Kim, H. J.; Son, J.; Park, H. J.; Lee, B. J.; and Hwang, T. S. Rice-husk flour filled polypropylene composites; mechanical and morphological study. Composite Structures 63 (2004) : 305-312.
- [46] Premalal, H. G. B.; Ismail, H. and Baharin. A. Comparison of the mechanical properties of rice husk powder filled polypropylene composites with talc filled polypropylene composites. Polymer Testing 21 (2002) : 833-839.
- [47] Garcia, D.; Lopez, J.; Balart, R.; Ruseckaite, R. A.; and Stefani P. M. Composites based on sintering rice husk-waste tire rubber mixtures. Materials and Design 28 (2007) : 2234-2238.
- [48] Jangchud, I. Effects of Fiber Content and Plasticizer Loading on Mechanical Properties of Natural Rubber Fibers-PVC Composites. การประชุมการป่าไม้ ประจำปี 2545 ด้านวัสดุทดแทนไม้ (2545) : 100-107.]
- [49] Stark, N. M. and Berger, M. J. Effect of Particle Size on Properties of Wood-Flour Reinforced Polypropylene Composites. The Fourth International Conference on Woodfiber-Plastic Composites (1997) : 134-143.
- [50] Ismail, H.; Rozman, H. D.; Jaffri, R. M.; and Ishak, Z. A. M. Oil palm wood flour reinforced epoxidized natural rubber composites: The effect of filler content and size. Eur. Polym. J. 33 (1997) : 1627-1632.

- [51] Kim, Y. S.; Guo, G.; Wang, K. H.; and Park, C. B. The effects of a coupling agent on the structure and on the property of stretched PP/wood-fiber composites-based artificial wood. Foams (2004).
- [52] Suarez, J. C. M.; Coutinho, F.M.B. and Sydenstricker, T.H. SEM studies of tensile fracture surfaces of polypropylene-sawdust composites. Polymer Testing 22 (2003) : 819–824.
- [53] Zheng, Y. T.; Cao, D. R.; Wang, D. S.; and Chen, J. J. Study on the interface modification of bagasse fibre and the mechanical properties of its composite with PVC. Composites: Part A 38 (2007) : 20-25.
- [54] Zhu, A.; Cai, A.; Zhou, W.; and Shi, Z. Effect of flexibility of grafted polymer on the morphology and property of nanosilica/PVC composites. Applied Surface Science (2007).
- [55] ASTM D 638 – 03 Standard Test Method for Tensile Properties of Plastics, 2002.
- [56] ASTM D 695 – 02a Standard Test Method for Compressive Properties of Rigid Plastics, 2002.
- [57] ASTM D 648 – 06 Standard Test Method for Deflection Temperature of Plastics Under Flexural Load in the Edgewise Position, 2006.
- [58] ASTM D 570 – 98 Standard Test Method for Water Absorption of Plastics, 2005.
- [59] ASTM D 1435 Standard Practice for Outdoor Weathering of Plastics, 2005.
- [60] Wolcott, M. P. Production Methods and Platforms for Wood Plastic Composites. Civil and Environmental Engineering, Wood Materials and Engineering Laboratory, Washington State University.
- [61] Georgia Gulf 3014 Rigid PVC, Extrusion [Online], Available:
<http://www.matweb.com/search/DataSheet.aspx?MatID=41707>
[25 March 2008].
- [62] Georgia Gulf 3020 Rigid PVC, Extrusion [Online], Available:
<http://www.matweb.com/search/DataSheet.aspx?MatID=41656>
[25 March 2008].
- [63] Green, D. W.; Winandy, J. E. and Kretschmann, D. E. Wood handbook - Wood as an engineering material. Wisconsin : Forest Products Laboratory, 1999.
- [64] Cabonyx new innovation: Mechanical Properties [Online], Available:
<http://www.vpwood.com/home/pdf/cer.pdf> [25 March 2008].

- [65] Wan, C.; Qiao, X.; Zhang, Y.; and Zhang, Y. Effect of different clay treatment on morphology and mechanical properties of PVC-clay nanocomposites. Polymer Testing 22 (2003) : 453-461.
- [66] Ahmad, Z.; Al-Awadi, N. A. and Al-Sagheer, F. Thermal degradation studies in poly(vinyl chloride)/poly(methyl methacrylate) blends. Polymer Degradation and Stability 93 (2008) : 456-465.
- [67] Nawaplastic Industries Company Limited, Thailand.
- [68] Siam Power Supply Company Limited, Thailand.

APPENDIX

Appendix

Mechanical and Physical Characterizations

Appendix 1 Tensile modulus of the PVC/RHA composites.

Particle size (μm)	Tensile modulus (GPa)			
	20 phr	40 phr	60 phr	80 phr
45	2.08 \pm 0.03	2.30 \pm 0.08	2.54 \pm 0.07	2.62 \pm 0.05
75	2.09 \pm 0.05	2.30 \pm 0.06	2.57 \pm 0.05	2.60 \pm 0.07
106	2.04 \pm 0.07	2.28 \pm 0.06	2.55 \pm 0.04	2.65 \pm 0.07
180	2.08 \pm 0.06	2.26 \pm 0.05	2.53 \pm 0.02	2.59 \pm 0.13
250	2.07 \pm 0.04	2.30 \pm 0.02	2.48 \pm 0.10	2.62 \pm 0.02

Tensile modulus of the PVC compound is 1.72 \pm 0.05 GPa.

Appendix 2 Tensile strength of the PVC/RHA composites.

Particle size (μm)	Tensile strength (MPa)			
	20 phr	40 phr	60 phr	80 phr
45	33.62 \pm 0.20	31.06 \pm 1.13	25.63 \pm 0.40	22.68 \pm 0.46
75	33.61 \pm 0.74	31.26 \pm 0.70	25.74 \pm 0.56	21.50 \pm 1.08
106	32.93 \pm 0.85	31.25 \pm 0.40	25.64 \pm 0.43	23.33 \pm 0.78
180	33.28 \pm 0.51	30.36 \pm 0.58	25.54 \pm 0.37	22.17 \pm 1.23
250	33.14 \pm 0.98	30.36 \pm 0.34	24.98 \pm 0.58	22.64 \pm 0.75

Tensile strength of the PVC compound is 39.04 \pm 0.62 MPa.

Appendix 3 Flexural modulus of the PVC/RHA composites.

Particle size (μm)	Flexural modulus (GPa)			
	20 phr	40 phr	60 phr	80 phr
45	2.57 \pm 0.06	2.72 \pm 0.05	3.01 \pm 0.12	3.60 \pm 0.07
75	2.57 \pm 0.04	2.69 \pm 0.06	3.13 \pm 0.13	3.63 \pm 0.06
106	2.54 \pm 0.03	2.72 \pm 0.05	3.07 \pm 0.04	3.58 \pm 0.19
180	2.50 \pm 0.02	2.71 \pm 0.06	3.08 \pm 0.07	3.55 \pm 0.26
250	2.51 \pm 0.06	2.71 \pm 0.06	3.04 \pm 0.08	3.54 \pm 0.31

Flexural modulus of the PVC compound is 2.11 \pm 0.26 GPa.

Appendix 4 Flexural strength of the PVC/RHA composites.

Particle size (μm)	Flexural strength (MPa)			
	20 phr	40 phr	60 phr	80 phr
45	40.55 \pm 0.63	38.86 \pm 1.01	38.99 \pm 1.12	37.54 \pm 0.30
75	40.01 \pm 1.33	38.43 \pm 0.88	37.69 \pm 0.77	37.64 \pm 0.39
106	39.79 \pm 0.32	38.31 \pm 0.54	38.20 \pm 0.49	37.32 \pm 1.00
180	39.76 \pm 0.24	37.80 \pm 0.53	38.31 \pm 0.73	36.79 \pm 1.89
250	40.10 \pm 0.57	37.64 \pm 0.24	38.21 \pm 0.44	37.28 \pm 0.88

Flexural strength of the PVC compound is 44.07 \pm 3.81 GPa.

Appendix 5 Compressive modulus of the PVC/RHA composites.

Particle size (μm)	Compressive modulus (GPa)			
	20 phr	40 phr	60 phr	80 phr
45	1.74 \pm 0.13	2.12 \pm 0.15	2.25 \pm 0.04	2.40 \pm 0.08
75	1.71 \pm 0.12	2.02 \pm 0.07	2.21 \pm 0.12	2.33 \pm 0.45
106	1.66 \pm 0.08	2.00 \pm 0.12	2.15 \pm 0.06	2.35 \pm 0.10
180	1.57 \pm 0.07	1.98 \pm 0.11	2.20 \pm 0.16	2.36 \pm 0.15
250	1.58 \pm 0.06	1.95 \pm 0.08	2.25 \pm 0.07	2.32 \pm 0.23

Compressive modulus of the PVC compound is 1.33 \pm 0.08 GPa.

Appendix 6 Compressive strength of the PVC/RHA composites.

Particle size (μm)	Compressive strength (MPa)			
	20 phr	40 phr	60 phr	80 phr
45	46.02 \pm 1.33	52.96 \pm 0.66	53.74 \pm 2.26	60.08 \pm 3.10
75	44.42 \pm 1.36	51.02 \pm 1.56	53.20 \pm 1.46	57.85 \pm 1.19
106	43.87 \pm 1.07	48.06 \pm 2.92	54.39 \pm 0.69	60.28 \pm 2.18
180	43.22 \pm 1.67	49.83 \pm 1.70	52.72 \pm 1.65	57.48 \pm 3.79
250	44.87 \pm 1.14	50.27 \pm 1.91	53.08 \pm 0.76	60.68 \pm 2.29

Compressive strength of the PVC compound is 37.50 \pm 1.73 MPa.

Appendix 7 Notched Izod impact strength of the PVC/RHA composites.

Particle size (μm)	Notched Izod impact strength (kJ/m^2)			
	20 phr	40 phr	60 phr	80 phr
45	8.75 \pm 0.97	7.50 \pm 0.35	6.95 \pm 0.19	6.44 \pm 0.20
75	9.00 \pm 0.30	7.54 \pm 0.16	7.18 \pm 0.20	6.50 \pm 0.19
106	9.63 \pm 0.30	7.63 \pm 0.12	7.17 \pm 0.39	6.58 \pm 0.23
180	9.75 \pm 0.69	7.64 \pm 0.31	7.27 \pm 0.34	7.14 \pm 0.19
250	9.97 \pm 0.43	7.64 \pm 0.36	7.37 \pm 0.33	7.21 \pm 0.19

Notched Izod impact strength of the PVC compound is 12.10 \pm 0.55 kJ/m^2 .

Appendix 8 Density of the PVC/RHA composites.

Particle size (μm)	Density (g/cm^3)			
	20 phr	40 phr	60 phr	80 phr
45	1.471 \pm 0.002	1.507 \pm 0.002	1.552 \pm 0.003	1.584 \pm 0.002
75	1.470 \pm 0.002	1.511 \pm 0.002	1.549 \pm 0.002	1.586 \pm 0.004
106	1.461 \pm 0.001	1.497 \pm 0.006	1.552 \pm 0.003	1.577 \pm 0.005
180	1.461 \pm 0.001	1.503 \pm 0.007	1.549 \pm 0.002	1.571 \pm 0.005
250	1.456 \pm 0.007	1.482 \pm 0.004	1.545 \pm 0.003	1.569 \pm 0.002

Density of the PVC compound and RHA is 1.425 and 1.93 g/cm^3 respectively.

Appendix 9 Water absorption of the PVC/RHA composites.

Particle size (μm)	Water absorption (%)			
	20 phr	40 phr	60 phr	80 phr
45	0.44 \pm 0.04	0.56 \pm 0.02	0.93 \pm 0.07	1.15 \pm 0.08
75	0.42 \pm 0.01	0.56 \pm 0.01	0.90 \pm 0.04	1.16 \pm 0.05
106	0.47 \pm 0.03	0.69 \pm 0.03	1.00 \pm 0.05	1.22 \pm 0.03
180	0.51 \pm 0.02	0.72 \pm 0.02	1.04 \pm 0.03	1.33 \pm 0.02
250	0.53 \pm 0.02	0.77 \pm 0.03	1.04 \pm 0.03	1.35 \pm 0.05

Water absorption of the PVC compound is 1.16 \pm 0.11 %.

VITA

Mr. Veerachai Kiet-udomphan was born in Bangkok, Thailand on March 1, 1984. He completed senior high school from Chinorotwittayalai School of Bangkok, Thailand in 2002. In 2006, he received Bachelor's Degree of Chemical Engineering from Mahidol University, Nakornpathom, Thailand. After graduation, he immediately pursued his graduate study for a Master's Degree in Chemical Engineering at the Department of Chemical Engineering, Faculty of Engineering, Chulalongkorn University, Bangkok, Thailand.